



# Modulation of Titin-Based Stiffness in Hypertrophic Cardiomyopathy via Protein Kinase D

Melissa Herwig<sup>1,2,3,4†</sup>, Detmar Kolijn<sup>1,2,3,4†</sup>, Mária Lódi<sup>1,2,3,5,6</sup>, Soraya Hölper<sup>7</sup>, Árpád Kovács<sup>1,2,3</sup>, Zoltán Papp<sup>5</sup>, Kornelia Jaquet<sup>1,2,3</sup>, Peter Haldenwang<sup>8</sup>, Cris Dos Remedios<sup>9</sup>, Peter H. Reusch<sup>3</sup>, Andreas Mügge<sup>1,2</sup>, Marcus Krüger<sup>10,11</sup>, Jens Fielitz<sup>12,13</sup>, Wolfgang A. Linke<sup>14</sup> and Nazha Hamdani<sup>1,2,3,4\*</sup>

<sup>1</sup> Department of Molecular and Experimental Cardiology, Ruhr University Bochum, Bochum, Germany, <sup>2</sup> Department of Cardiology, St. Josef-Hospital, Ruhr University Bochum, Bochum, Germany, <sup>3</sup> Department of Clinical Pharmacology, Ruhr University Bochum, Bochum, Germany, <sup>4</sup> Institute of Physiology, Ruhr University Bochum, Bochum, Germany, <sup>5</sup> Division of Clinical Physiology, Department of Cardiology, Faculty of Medicine, University of Debrecen, Debrecen, Hungary, <sup>6</sup> Kálmán Laki Doctoral School, University of Debrecen, Debrecen, Hungary, <sup>7</sup> Sanofi-Aventis Deutschland GmbH Industriepark Höchst, Frankfurt, Germany, <sup>8</sup> Department of Cardiothoracic Surgery, University Hospital Bergmannsheil Bochum, Bochum, Germany, <sup>9</sup> School of Medical Sciences, Bosch Institute, University of Sydney, Camperdown, NSW, Australia, <sup>10</sup> Institute for Genetics, Cologne Excellence Cluster on Cellular Stress Responses in Aging-Associated Diseases, Cologne, Germany, <sup>11</sup> Center for Molecular Medicine (CMMC), University of Cologne, Cologne, Germany, <sup>12</sup> Department of Internal Medicine B, Cardiology, University Medicine Greifswald, Greifswald, Germany, <sup>13</sup> DZHK (German Center for Cardiovascular Research), Partner Site Greifswald, Greifswald, Germany, <sup>14</sup> Institute of Physiology II, University Hospital Münster, University of Münster, Münster, Germany

## OPEN ACCESS

### Edited by:

Sachio Morimoto,  
International University of Health and  
Welfare (IUHW), Japan

### Reviewed by:

Miklos Kellermayer,  
Semmelweis University, Hungary  
Joseph D. Powers,  
University of California, San Diego,  
United States

### \*Correspondence:

Nazha Hamdani  
nazha.hamdani@rub.de

†These authors have contributed  
equally to this work

### Specialty section:

This article was submitted to  
Striated Muscle Physiology,  
a section of the journal  
Frontiers in Physiology

Received: 19 December 2019

Accepted: 02 March 2020

Published: 15 April 2020

### Citation:

Herwig M, Kolijn D, Lódi M, Hölper S,  
Kovács Á, Papp Z, Jaquet K,  
Haldenwang P, Dos Remedios C,  
Reusch PH, Mügge A, Krüger M,  
Fielitz J, Linke WA and Hamdani N  
(2020) Modulation of Titin-Based  
Stiffness in Hypertrophic  
Cardiomyopathy via Protein Kinase D.  
Front. Physiol. 11:240.  
doi: 10.3389/fphys.2020.00240

The giant protein titin performs structure-preserving functions in the sarcomere and is important for the passive stiffness ( $F_{\text{passive}}$ ) of cardiomyocytes. Protein kinase D (PKD) enzymes play crucial roles in regulating myocardial contraction, hypertrophy, and remodeling. PKD phosphorylates myofilament proteins, but it is not known whether the giant protein titin is also a PKD substrate. Here, we aimed to determine whether PKD phosphorylates titin and thereby modulates cardiomyocyte  $F_{\text{passive}}$  in normal and failing myocardium. The phosphorylation of titin was assessed in cardiomyocyte-specific PKD knock-out mice (cKO) and human hearts using immunoblotting with a phosphoserine/threonine and a phosphosite-specific titin antibody. PKD-dependent site-specific titin phosphorylation *in vivo* was quantified by mass spectrometry using stable isotope labeling by amino acids in cell culture (SILAC) of SILAC-labeled mouse heart protein lysates that were mixed with lysates isolated from hearts of either wild-type control (WT) or cKO mice.  $F_{\text{passive}}$  of single permeabilized cardiomyocytes was recorded before and after PKD and HSP27 administration. All-titin phosphorylation was reduced in cKO compared to WT hearts. Multiple conserved PKD-dependent phosphosites were identified within the Z-disk, A-band and M-band regions of titin by quantitative mass spectrometry, and many PKD-dependent phosphosites detected in the elastic titin I-band region were significantly decreased in cKO. Analysis of titin site-specific phosphorylation showed unaltered or upregulated phosphorylation in cKO compared to matched WT hearts.  $F_{\text{passive}}$  was elevated in cKO compared to WT cardiomyocytes and PKD administration lowered  $F_{\text{passive}}$  of WT and cKO cardiomyocytes. Cardiomyocytes from hypertrophic cardiomyopathy (HCM) patients showed higher  $F_{\text{passive}}$  compared to control hearts and significantly lower  $F_{\text{passive}}$  after PKD treatment. In addition, we found higher phosphorylation at CaMKII-dependent titin sites in HCM compared to control hearts. Expression and phosphorylation of HSP27,

a substrate of PKD, were elevated in HCM hearts, which was associated with increased PKD expression and phosphorylation. The relocalization of HSP27 in HCM away from the sarcomeric Z-disk and I-band suggested that HSP27 failed to exert its protective action on titin extensibility. This protection could, however, be restored by administration of HSP27, which significantly reduced  $F_{\text{passive}}$  in HCM cardiomyocytes. These findings establish a previously unknown role for PKD in regulating diastolic passive properties of healthy and diseased hearts.

**Keywords:** titin, HCM, PKD, Hsp27, stiffness

## INTRODUCTION

Protein kinase (PK)D is a serine/threonine kinase that belongs to the family of calcium/calmodulin-dependent kinases (CaMKII) due to its catalytic domain structure and substrate specificity. The PKD kinase family consists of three members: PKD1 (formerly known as PKC $\mu$ ) (Valverde et al., 1994) and the predominant isoforms in the heart (Sin and Baillie, 2012), PKD2 (Sturany et al., 2001), and PKD3 (also known as PKC $\nu$ ) (Hayashi et al., 1999). The isoforms differ in structural and enzymatic properties from members of the PKC family. Some substrates that are targets of PKC are not phosphorylated by PKD (Johannes et al., 1994; Valverde et al., 1994; Van Lint et al., 1995), and unlike CaMKII, PKD is not directly activated by  $\text{Ca}^{2+}$  or calmodulin (Avkiran et al., 2008).

PKD can be activated by other stimuli including reactive oxygen species (ROS), growth factors (i.e., platelet-derived growth factor), and triggering of immune cell receptors. The PKD kinase is involved in the regulation of myocardial contraction by phosphorylating cardiac myosin binding protein C (cMyBP-C), cardiac troponin I (cTnI) and the L-type, voltage gated  $\text{Ca}^{2+}$  channel (Haworth et al., 2004; Cuello et al., 2007; Aita et al., 2011; Dirkx et al., 2012). Phosphorylation of TnI by PKD resulted in a significant rightward shift of the tension-pCa relationship, indicating reduced myofilament  $\text{Ca}^{2+}$  sensitivity (Haworth et al., 2004; Cuello et al., 2007; Aita et al., 2011; Dirkx et al., 2012). At submaximal  $\text{Ca}^{2+}$  activation, PKD-mediated phosphorylation also accelerated isometric cross-bridge cycling kinetics (Haworth et al., 2004; Cuello et al., 2007), suggesting a beneficial effect of PKD activation on cardiac function. PKD also alters gene expression leading to hypertrophy and influencing cardiac remodeling processes (Vega et al., 2004; Harrison et al., 2006).

With a molecular mass ranging from 3,000 to 3,700 kDa, titin is the largest known protein and its function as a molecular spring is important for the elasticity of striated muscle. Spanning the half-sarcomere from the Z-disk to the M-band, titin is expressed in various isoforms that confer different elastic properties to the sarcomere. Two main isoform classes of titin are expressed in the human heart: a shorter, stiffer N2B (3,000 kDa) isoform and several longer, more compliant, N2BA isoforms (>3,200 kDa). These variants differ in their elastic I-band region due to alternative splicing, whereas the Z-disk, A-band, and M-band regions of titin are essentially constitutively expressed. The titin spring region has a complex sequence comprising two types of

extensible segments: (1) regions composed of immunoglobulin-like (Ig-) domains (proximal; middle; distal) arranged in tandem; and (2) intrinsically disordered structures, including a unique sequence of the cardiac specific “N2-B” element (“N2-Bus”) and the “PEVK” segment rich in proline, glutamate, valine, and lysine.

The titin filaments in cardiomyocytes are considered to be a main determinant of myocardial “passive” stiffness, along with the collagen fibers of the extracellular matrix and additional factors such as diastolic  $\text{Ca}^{2+}$  levels. We have previously demonstrated that the stiffness of cardiac titin is highly variable and depends on titin isoform switching and/or post-translational modifications such as phosphorylation and oxidation (Linke and Hamdani, 2014).

In our previous study, using a CaMKII knockout mouse model together with the stable isotope labeling of amino acids in cell culture (SILAC) mouse model, we found ~20 CaMKII-dependent phosphosites along the titin molecule (Hamdani et al., 2013b). Some phosphosites were located within the extensible region of titin, e.g., at the N2-Bus and PEVK spring elements, while others were within the A-band, M-band, and Z-disk regions of titin. Using this approach, we also detected >50 additional titin phosphosites that appeared to be not regulated by CaMKII. As regards to other kinases, protein kinase A and G and ERK2 were shown to phosphorylate the titin springs at specific sites within the cardiac-specific N2-Bus element (Kruger et al., 2009; Kotter et al., 2013). This modification alters the molecular stiffness of N2-Bus. Yet another kinase, PKC $\alpha$ , was shown to phosphorylate titin’s PEVK element (Hidalgo et al., 2009).

A well-known substrate of PKD, among others, is heat shock protein 27 (HSP27) (Doppler et al., 2005). HSPs are molecular chaperones comprising a large family of proteins involved in protection against various forms of cellular stress (Mymrikov et al., 2011). HSPs generally facilitate protein refolding, target misfolded proteins to the proteasome and stabilize and transport partially folded proteins to different cellular compartments. Under various environmental insults such as heat, oxidative stress or acidosis, protein denaturation occurs and leads to unfolding and undesirable protein aggregates (Mymrikov et al., 2011). HSP27 is a small (ATP-independent) HSP whose function is regulated, in part, by posttranslational modifications, including phosphorylation at Ser-18, Ser-78, Ser-82, and Thr-143 (Kostenko and Moens, 2009; Mymrikov et al., 2011). Previous work showed that the unfolded Ig regions of I-band titin, but not the intrinsically disordered segments, can aggregate, causing high titin-dependent myocyte stiffness,

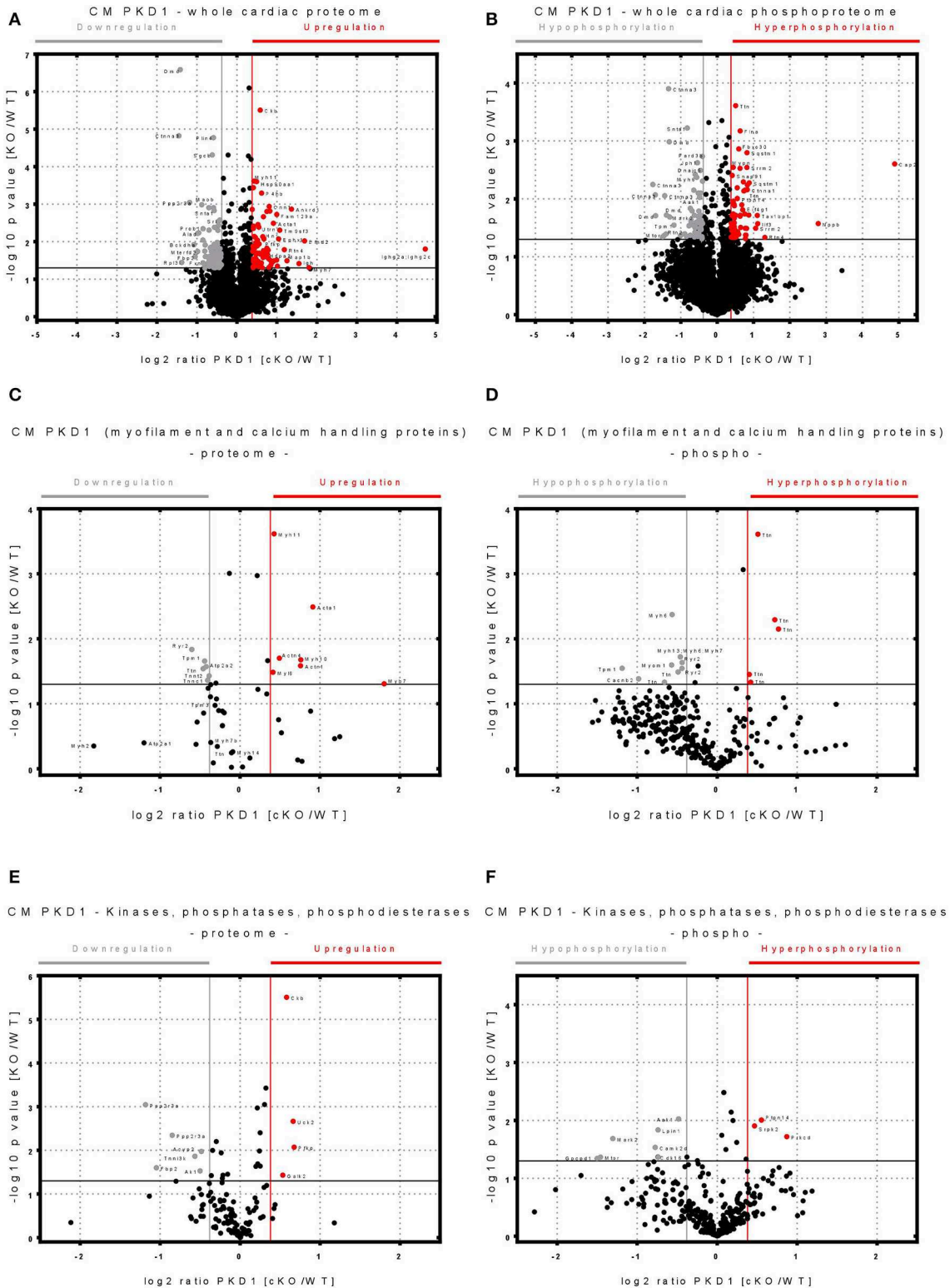


**FIGURE 1** | Volcano plots showing changes in the cardiac proteome and phosphoproteome in protein kinase D 1 (PKD1)-cKO and matched wild-type (WT) mouse hearts. **(A)** Volcano plot of whole cardiac proteome with identified significantly up- or down-regulated peptides in wild type (WT) vs. cardiomyocyte specific Protein Kinase D1 (PKD1) knock-out (KO) animals. **(B)** Volcano plot of whole cardiac phosphoproteome with identified significantly hyper- or hypo-phosphorylated peptides in WT vs. PKD1 cKO mice.

(Continued)

**FIGURE 1 | (C)** Volcano plot of myofilament and calcium handling proteins with significantly up- or down-regulated peptides in WT vs. PKD1 cKO mice. **(D)** Volcano plot of myofilament and calcium handling proteins with significantly hyper- or hypo-phosphorylated peptides in WT vs. PKD1 cKO mice. **(E)** Volcano plot of kinases, phosphatases, phosphodiesterases identified with significantly up- or down-regulated peptides in WT vs. PKD1 cKO mice. **(F)** Volcano plot of kinases, phosphatases, phosphodiesterases identified with significantly hyper- or hypo-phosphorylated peptides in WT vs. PKD1 cKO mice. Protein content or phosphorylation considered as significantly changed ( $-\log_{10} p \geq 1.3$ ,  $\log_2 \text{ratio} \geq \pm 0.37$ ) over the WT are color-coded. Only values with  $-\log_{10} p > 0$  are shown. Experiments were performed in triplicates.

and that HSP27 prevented this aggregation and suppressed the stiffening (Kotter et al., 2014). We speculated that cardiomyocyte elastic function could be protected under stress, at least in part, by HSP27 being regulated via PKD-mediated phosphorylation. The main aim of the present study was to investigate the effects of PKD on titin phosphorylation *in vivo* and resulting functional changes using cardiomyocyte specific *Prkd1*, which encodes for PKD1, knockout mice, SILAC mouse hearts, and human hypertrophic cardiomyopathy (HCM) heart tissues. We identified various PKD1-dependent phosphosites within titin using quantitative mass spectrometry (MS) and showed that PKD1-mediated titin-phosphorylation reduces cardiomyocyte  $F_{\text{passive}}$ . Additionally, we found increased oxidative stress in human HCM tissues along with increased HSP27 expression and phosphorylation. HCM tissues also showed increased CaMKII-dependent phosphorylation at the PEVK and N2Bus titin regions. High cardiomyocyte stiffness was corrected by incubation with HSP27 and PKD, probably through relief of titin aggregation. Taken together, our results highlight the important roles of PKD and HSP27, in the presence of oxidative stress, in modulating diastolic function via titin-based stiffness regulation.

## METHODS

Detailed methods descriptions are provided in the online **Supplementary Methods**.

### Human Heart Tissues

The investigation conforms to the principles outlined in the Declaration of Helsinki and samples were obtained after informed consent and with approval of the local Ethics Committee. LV tissue was obtained from end-stage heart failure patients (NYHA III or IV;  $n = 10$ ), hypertrophic cardiomyopathy (male, mean age 45 years). LV tissue from non-failing donor hearts ( $N = 10$ ;  $\pm$  40 years of age) served as reference and was obtained from donor hearts ( $n = 5$ ).

### Cardiomyocyte Specific *Prkd1* Knock-Out Mice

All animal procedures were performed in accordance with the guidelines of Charité Universitätsmedizin Berlin as well as Max-Delbrück Center for Molecular Medicine and were approved by the Landesamt für Gesundheit und Soziales (LaGeSo, Berlin, Germany) for the use of laboratory animals (permit number: G 0229/11) and followed the 'Principles of Laboratory Animal Care' (NIH publication no. 86-23, revised 1985) as well as the current version of German Law on the Protection of Animals. The generation and usage of the conditional *Prkd1* allele was published elsewhere (Fielitz

et al., 2008; Kim et al., 2008). The Cre-loxP recombination system was used for the generation of a conditional *Prkd1* allele. *Prkd1loxP/loxP* mice were crossed with Cre carrying mice controlled by cardiomyocyte-specific alpha-myosin-heavy-chain promoter ( $\alpha$ MHC-Cre) (Agah et al., 1997) (cKO, *Prkd1loxP/loxP*;  $\alpha$ MHC-Cre).  $\alpha$ MHC-Cre-negative littermates were used as controls (WT, *Prkd1loxP/loxP*). Cardiac tissue was obtained when mice were 8–10 weeks of age.  $N = 7$  for both KO and WT.

### SILAC-Based Quantitative Mass Spectrometry

We mixed equal amounts of protein lysates from heart tissue (7.5 mg) from the 13Lys6 heavy-labeled SILAC mouse and a non-labeled WT or non-labeled *Prkd1* cKO mouse. After protein digestion and phosphopeptide enrichment, the ratio of labeled:unlabeled peptides was determined by liquid chromatography and tandem MS and used to identify the cKO:WT ratio of titin phosphopeptides (Kruger et al., 2008).

### Titin Isoform Separation

Homogenized myocardial samples were analyzed by 1.8% SDS-PAGE. Protein bands were visualized by Coomassie staining and analyzed densitometrically.

### All-Titin Phosphorylation Assays

Titin bands were stained with anti-phospho-antibody directed against phospho-serine/threonine. Phospho-protein signals were indexed to total-protein signals and normalized to the intensity of coomassie staining to correct for differences in sample loading. Alternatively, all-titin phosphorylation was measured by PKD-mediated back-phosphorylation (Hamdani et al., 2013b).

### Titin and Phosphotitin Western Blots

Western blots were performed using custom-made, affinity-purified, anti-phosphoserine-specific antibodies directed against phospho-Ser-4010, -Ser-4062, -Ser-4099 (all N2Bus), -Ser-11878, and -Ser-12022 (both PEVK), of human titin (UniProtKB identifier, Q8WZ42), and antibodies recognizing the corresponding nonphosphorylated sequence at these sites (Hamdani et al., 2013b). We also used phosphosite-specific antibodies against phospho-Ser-3991, -Ser-4043, -Ser-4080 (all N2Bus), -Ser-12742, and -Ser-12884 (both PEVK), of mouse titin (UniProtKB identifier, A2ASS6) (Hamdani et al., 2013b).

### Force Measurements on Isolated Cardiomyocytes

Cardiomyocytes were skinned and single isolated cells ( $n = 12$ –42/5–6 heart/group) attached between a force transducer and

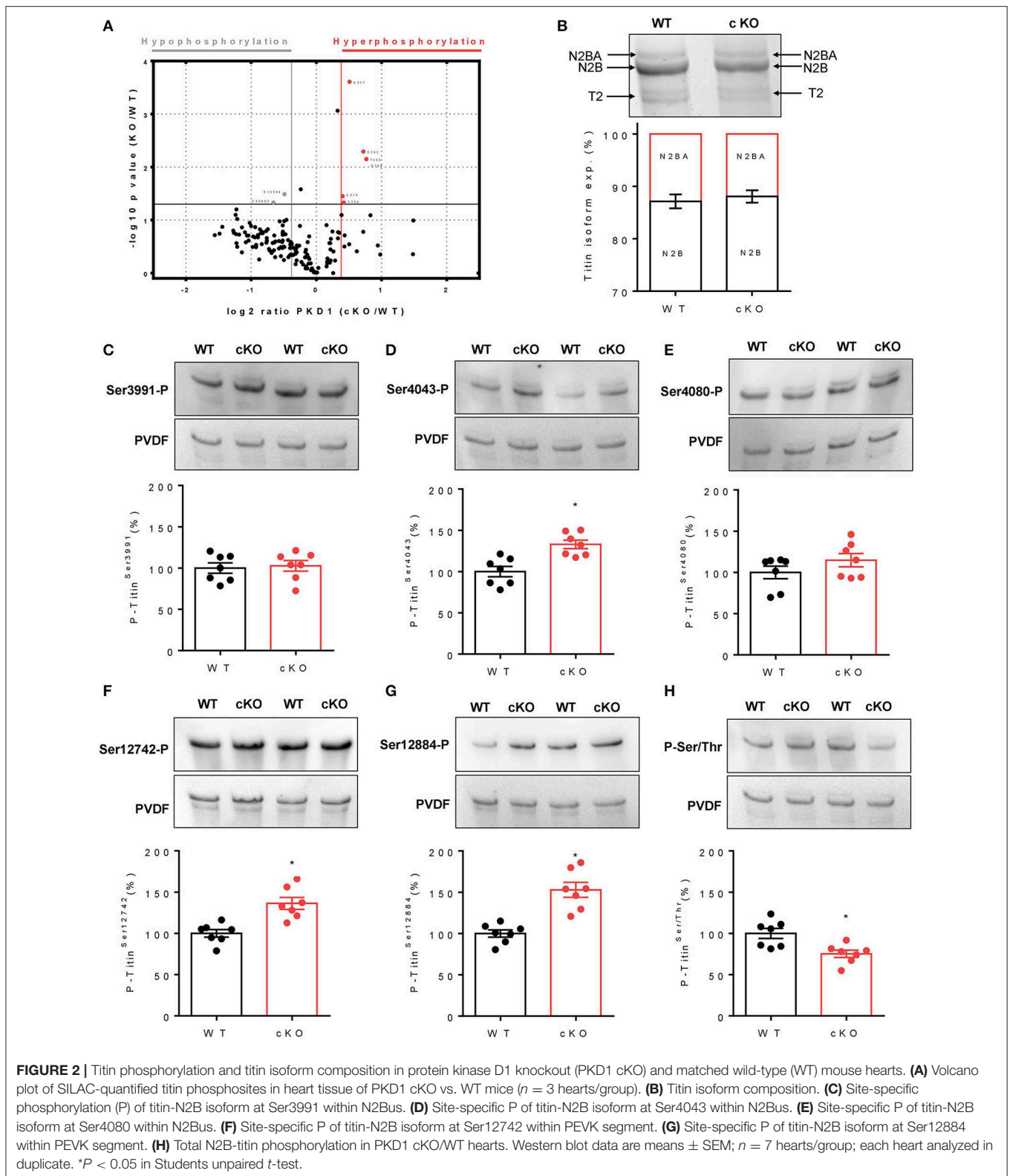


**FIGURE 2 |** Titin phosphorylation and titin isoform composition in protein kinase D1 knockout (PKD1 cKO) and matched wild-type (WT) mouse hearts. **(A)** Volcano plot of SILAC-quantified titin phosphosites in heart tissue of PKD1 cKO vs. WT mice ( $n = 3$  hearts/group). **(B)** Titin isoform composition. **(C)** Site-specific phosphorylation (P) of titin-N2B isoform at Ser3991 within N2Bus. **(D)** Site-specific P of titin-N2B isoform at Ser4043 within N2Bus. **(E)** Site-specific P of titin-N2B isoform at Ser4080 within N2Bus. **(F)** Site-specific P of titin-N2B isoform at Ser12742 within PEVK segment. **(G)** Site-specific P of titin-N2B isoform at Ser12884 within PEVK segment. **(H)** Total N2B-titin phosphorylation in PKD1 cKO/WT hearts. Western blot data are means  $\pm$  SEM;  $n = 7$  hearts/group; each heart analyzed in duplicate. \* $P < 0.05$  in Students unpaired  $t$ -test.

motor (Hamdani et al., 2013a,b).  $F_{\text{passive}}$  was recorded over the sarcomere length (SL) range, 1.8–2.4  $\mu\text{m}$ , and was measured before/after PKD and/or HSP27 incubation.

### Quantification of Tissue Oxidative Stress

Myocardial levels ( $n = 7$  LV sample/group) of oxidative stress markers were tested with enzyme-linked immunosorbent assay

**TABLE 1** | Significantly changed titin phosphosites ( $-\log_{10} p\text{-value KO/WT} > 1.3$ ).

Position within titin	UniProt identifier	Log2 ratio (KO/WT)	$-\log_{10} p\text{-value KO/WT}$	Charge	Multiplicity	Localization probability	Classification of phosphosite	Sequence window
S33880	A2ASS6	-0.659036	1.33033	3	1	1	Class 1	DLYYYRRRRRSLGDMSEDELLLPIDDYLMK
S264	A2ASS6	0.419615	1.33152	2	2	1	Class 1	PHKTPPRIPPKPKRSPTPPSIAAKAQLARQ
S315	A2ASS6	0.40279	1.45166	2	1	0.997856	Class 1	PSPVRSVSPAGRISTSPIRSVKSPILLIRKIQ
S16544	A2ASS6	-0.489219	1.48858	3	1	0.993809	Class 1	AEEEEPFSLPLTERLSINNSKQGESQLRIRD
S20332	A2ASS6	-0.239112	1.58029	2	1	1	Class 1	IIGYVEMRPKIADASPDEGWKRCNAAAQLI
S264	A2ASS6	0.767076	2.14935	2	3	1	Class 1	PHKTPPRIPPKPKRSPTPPSIAAKAQLARQ
T266	A2ASS6	0.767076	2.14935	2	3	1	Class 1	KTPPRIPPKPKRSPTPPSIAAKAQLARQQS
S262	A2ASS6	0.720452	2.29218	2	3	1	Class 1	QLPHKTPPRIPPKPKRSPTPPSIAAKAQLA
S322	A2ASS6	0.325277	3.06343	2	1	1	Class 1	SPAGRISTSPIRSVKSPILLIRKQTITMATG
S307	A2ASS6	0.509144	3.60898	2	2	1	Class 1	VRHVRAPTSPVRSVSPAGRISTSPIRSVKS

Z-disk.

A-band.

M-band.

Multiplicity contains information about the phosphorylation of the peptides (single, double, triply phosphorylated).

**TABLE 2** | Detected phosphosites in the elastic I band titin spring ( $-\log_{10} p\text{-value KO/WT} > 0$ ).

Position within titin	UniProt identifier	Log2 ratio (KO/WT)	$-\log_{10} p\text{-value KO/WT}$	Charge	Multiplicity	Localization probability	Classification of phosphosite	Sequence window
T9146	A2ASS6	-0.650309	0.429695	3	1	0.616703	Class 2	KERLIPPSFTKKLSETVEETEGNSFKLEGRV
S3286	A2ASS6	-0.938293	0.866542	2	1	0.851679	Class 1	RPQPKISWYKEEQLLSTGFKCKFLHDGQEYT
S3977	A2ASS6	-0.319098	0.36361	2	1	0.840288	Class 1	CTEGKILMASADTLKSTGQDVALRTEEGKSL
T13665	A2ASS6	-0.316873	0.41921	2	1	1	Class 1	CEVSREPKTFRWLKGTQEITGDDRFELIKDG
S13228	A2ASS6	-0.273069	0	2	1	0.993076	Class 1	DIPGEWKLKGELLRPSPTCEIAEGGKRFLLT
S9201	A2ASS6	-0.230981	0	2	1	1	Class 1	IMFKNNALLLQVKRAMADAGLYTCKATNDA
S9144	A2ASS6	-0.203903	0.163212	2	1	1	Class 1	NIKERLIPPSFTKKLSETVEETEGNSFKLEG
S4175	A2ASS6	-0.168399	0.396358	3	1	1	Class 1	HEEDKIDVQGGRRDHLSDAQKVVETVIEAEADS
T14268	A2ASS6	-0.16409	0.087451	2	1	0.99985	Class 1	VFTKNLANLEVSEGDTIKLVCEVSKPGAIEVI
S9459	A2ASS6	-0.158813	0.124587	3	1	1	Class 1	DLRAMLKKTPALKKSGSEEEIDIMELLKNV
S13204	A2ASS6	-0.0662166	0.089154	2	1	0.880947	Class 1	LKPIEDVTIYEKESASFDAEISEEDIPGEWK
S4018	A2ASS6	-0.018641	0	2	1	0.675564	Class 2	VLLKEEQSEWVAVPTSQTSKSEKEPEAIKGV
S3991	A2ASS6	-0.0149712	0.0107483	2	1	0.999502	Class 1	KSTGQDVALRTEEGKSLSFPLALEEKQVLLK
S3870	A2ASS6	-0.00516502	0.0056415	3	1	0.991661	Class 1	EPEGVFPGASSAAQVSPVTIKPLITLTAEPK
S14664	A2ASS6	0.0113125	0.0110327	2	1	1	Class 1	REIKEGKYYKFEKDGSIHRLIKDCRLEDEC
S13764	A2ASS6	0.200173	0	2	1	1	Class 1	SWFKNDQRLHTSKRVSMHDEGKTHSITFKDL
S3676	A2ASS6	0.258327	0	4	1	0.878152	Class 1	EDMPLYTSVCYTIHSPDGSSTFVNDPQRG
S12678	A2ASS6	0.331543	0.65471	3	1	1	Class 1	IEKPKLKRPPARPPSPKEDVKEKMFQLKA
T10276	A2ASS6	0.395205	0	3	1	0.637793	Class 2	EVQKQVVEEKIAITQREESPPPAVPEIPK
S10281	A2ASS6	0.719508	0.777963	3	1	0.999995	Class 1	VVTEEKIAITQREESPPPAVPEIPKVVPE
S12871	A2ASS6	0.829341	1.09019	3	1	1	Class 1	AKPKGPIKGVAKKTPSPIEAERKLRPGSGG
S12884	A2ASS6	0.94305	0.52056	3	1	1	Class 1	TPSPIEAERKLRPGSGGKPPDEAPFTYQL
S12871	A2ASS6	0.981417	0.3495	3	2	1	Class 1	AKPKGPIKGVAKKTPSPIEAERKLRPGSGG
T12869	A2ASS6	0.981417	0.3495	3	2	1	Class 1	EAAKPKGPIKGVAKKTPSPIEAERKLRPGS

Proximal Ig region.

N2B-element.

Middle Ig region.

PEVK.

Distal Ig domains.

**TABLE 3** | Downregulated titin phosphosites (log<sub>2</sub> ratio KO/WT < -0.37).

Position within titin	UniProt identifier	Log <sub>2</sub> ratio (KO/WT)	-Log <sub>10</sub> p-value KO/WT	Charge	Multiplicity	Localization probability	Classification of phosphosite	Sequence window
S23560	A2ASS6	-0.372779	0	3	1	0.692852	Class 2	PGPPGNPRVLDTSRSSISIAWNKPIYDGGSE
S18225	A2ASS6	-0.376743	0.548646	2	1	0.5	Class 2	PPGPPFPKVDWTKSSVDLEWSPPLKDDGGSK
S30484	A2ASS6	-0.380153	0	2	1	0.999969	Class 1	TWKLEEMRLKETDRMSIATTKDRITTLTVKDS
S34451	A2ASS6	-0.384564	0.573934	2	1	0.999956	Class 1	TLTVQKARVIEKAVTSPPRVKSPEPRVKSPE
S33933	A2ASS6	-0.390718	0.578927	2	1	0.999999	Class 1	SRSPPRFELSSLRYSPPAHVKVEDRRRDFR
S34808	A2ASS6	-0.390976	0.349281	2	1	1	Class 1	IAEEVKRSAASLEKSIVHEEVTKTSQASEE
S26062	A2ASS6	-0.391391	0	3	1	0.992938	Class 1	KWSVVAESKVCNAWVSLGSSGQEQFRVKAY
S21726	A2ASS6	-0.391912	0.585051	2	1	0.999998	Class 1	FLTEENKQORVMKSLSLQYSTKDLKKEGKEYT
T27227	A2ASS6	-0.392365	0	3	1	0.598045	Class 2	QATVAWVKDGGVLRTRRVNVAASSKTVTLLS
S34476	A2ASS6	-0.399261	0.538309	2	1	1	Class 1	RVKSPETVKSPKRVKSPPEVTSHPKAVSPTTE
S28859	A2ASS6	-0.403171	0.471662	2	1	0.990318	Class 1	EPVAKNAFVTPGPPSIFEVTIKTKNSMTW
T4070	A2ASS6-3	-0.408659	0.331878	3	1	0.998519	Class 1	RELLSFPVEIQITAATPTPEQNKCEKRELFEL
S22271	A2ASS6	-0.42308	0	3	1	0.944504	Class 1	VSVLDVPGPPGPIEISNVSAEKATLWTWPPPL
S1196	A2ASS6	-0.429651	0.300969	3	1	0.887311	Class 1	ALVKTQQEMLYQTMSTFIQEPKVGEIAPGF
S29764	A2ASS6	-0.433024	0.621301	2	1	0.999999	Class 1	FGPEYFDGLVIKSGDSLRIKALVQGRVPRV
S26804	A2ASS6	-0.433475	0	3	1	0.524536	Class 2	LYPPGPPSNPKVTDTSRSSVSLAWNKPIYDG
S22184	A2ASS6	-0.435231	0	2	1	0.999983	Class 1	LDPTIKDGLTVKAGDSIVLSAISILGKPLPK
S28389	A2ASS6	-0.440064	0	2	1	0.999873	Class 1	ESVTLKWEPPKYDGGSHVTNYVILKRETSTA
S19152	A2ASS6	-0.442809	0	2	1	0.686958	Class 2	RKDVAQAQWVSLSTTSKSKSHMAKHLTEGNQ
S34292	A2ASS6	-0.458658	1.00349	2	1	0.997471	Class 1	LTKTEAYAVSSFKRTSELEAASSVREVKSQM
S848	A2ASS6	-0.472572	0.731925	2	1	0.999987	Class 1	ASIAGSAIATLQKELSATSTQKITKSVKAP
S19518	A2ASS6	-0.479462	0	3	1	0.999999	Class 1	DITENAATVSWTLPKSDGGSPITGYVERRE
T4827	A2ASS6-3	-0.480703	0	3	2	0.682593	Class 2	VRDTHKHAQLVQSDSTTSMEVEEVTFTVYE
S16544	A2ASS6	-0.489219	1.48858	3	1	0.993809	Class 1	AEEEEFPLPLTERLSINNSKQGESQLRIIRD
S29489	A2ASS6	-0.490109	0.49045	2	1	0.999929	Class 1	GGGEITCYSIEKREASQTNWKMVCSSVARTT
S35097	A2ASS6	-0.491363	0.979128	3	1	0.972789	Class 1	ESFVEMSSSSFMGKSSMTQLESSTSRMLKAG
S29997	A2ASS6	-0.496859	0.246525	3	1	0.999978	Class 1	KKSTRVWVKVSKRPISETFVKVTLGVEGNEY
S23358	A2ASS6	-0.498498	0.499119	3	1	0.855607	Class 1	RPGPPEGLAVSDVTSEKCVLSWLPPLDDGG
S262	A2ASS6	-0.501588	0	2	1	1	Class 1	QLPHKTPPRIPPKPKRSRPTPPSIAAKAQLA
S30452	A2ASS6	-0.513035	0.782215	2	1	0.968235	Class 1	DLTGITNQLITCKAGSTFTIDVPISGRPAK
S16548	A2ASS6	-0.515562	0.899345	3	1	0.999832	Class 1	EPFSLPLTERLSINNSKQGESQLRIIRSLRP
S24061	A2ASS6	-0.515855	0.613502	2	1	0.97456	Class 1	SVTLKWEPPKYDGGSSINNYVEKRDSTTITA
T23053	A2ASS6	-0.515985	0.758139	2	1	0.999999	Class 1	SVWANYPFKVPGPPGTPQVTA/TKDSMTISW
S1120	A2ASS6	-0.516292	0.722335	2	1	1	Class 1	CQIGGNPKPHVYWKSGVPLTTGYRYKVSYN
S21895	A2ASS6	-0.522994	0.473161	2	1	1	Class 1	EAMTLKWGPPKDDGGSEITNYVLEKRDSVNN
S34756	A2ASS6	-0.525721	0.586585	2	1	1	Class 1	VSTQKTSEVTSQKASAEQEEISQKALTSEEI
S21162	A2ASS6	-0.54349	0.319895	2	1	0.836052	Class 1	VNRKDSGDYITITAEENSSGSKSATIKLVLDK
S34778	A2ASS6	-0.543969	0.489795	2	1	0.999964	Class 1	QKALTSEEIKMSEVKSHETLAIKEEASKVLI
T22513	A2ASS6	-0.551522	0	3	1	0.958776	Class 1	VEHQKVGDDAWIKDITGTALRITQFVWPDQ
T24135	A2ASS6	-0.561529	0.975063	2	1	1	Class 1	PVWAQYPFKVPGPPGTPFVTLASKDSMEVQW
T23980	A2ASS6	-0.573932	0.604136	3	1	0.631224	Class 2	PPAVTWHKDDIPLKQTRRVNAESTENNSLLT
S21730	A2ASS6	-0.574432	0.464884	2	1	0.798102	Class 1	ENKWQRVMKSLSLQYSTKDLKKEGKEYTFRVS
S23609	A2ASS6	-0.587423	0	2	1	0.995346	Class 1	VTPPAGLKATSYTITSLIENQEYKIRIYAMN
S4650	A2ASS6-3	-0.606701	0	3	1	0.981316	Class 1	ALFQTPSADVEEANVSETGASVENGDKTFIS
T25062	A2ASS6	-0.625343	0	3	1	0.499999	Class 2	KPSISWTKDGMPLKQTRINVTDSLDTLLS
T25063	A2ASS6	-0.625343	0	3	1	0.499999	Class 2	PSISWTKDGMPLKQTRINVTDSLDTLLSI
S16620	A2ASS6	-0.62959	0.594816	3	1	0.999999	Class 1	DSVLCKWEPLDDGGSEIINYTLEKDKTKP
S25817	A2ASS6	-0.632049	0.301091	2	1	1	Class 1	VKPEDKLEAPELDLDELKRGIVRVAGGSAR
S34207	A2ASS6	-0.63678	0	2	1	0.992242	Class 1	AEVKWYHNGVELQESSKIHYTNTSGVLTLEI
S20215	A2ASS6	-0.644393	0.578427	2	1	0.989323	Class 1	EMTVWNAPEYDGGKSITGYLLEKKEKHAVR

(Continued)

TABLE 3 | Continued

Position within titin	UniProt identifier	Log2 ratio (KO/WT)	-Log 10 p-value KO/WT	Charge	Multiplicity	Localization probability	Classification of phosphosite	Sequence window
T30560	A2ASS6	-0.645399	0.70904	2	1	1	Class 1	ESCVL <sup>SWTEPKDDGGTEITNYIVEK</sup> RESGTT
T9146	A2ASS6	-0.650309	0.429695	3	1	0.616703	Class 2	KERLIPPSFTKKLSETVEETEGNSFKLEGRV
S33880	A2ASS6	-0.659036	1.33033	3	1	1	Class 1	DLYYYRRRRRSLGDM <sup>SDELLLPID</sup> DYLAMK
S21163	A2ASS6	-0.662774	0	2	1	0.555375	Class 2	NRKDSGDYTTAENS <sup>SGSKSATIKL</sup> KVLDPK
S32940	A2ASS6	-0.669661	0.567747	3	1	0.991067	Class 1	DSVNL <sup>TWTEPASDGGSKVTNYIVEK</sup> CATTAE
T27381	A2ASS6	-0.676248	0.40741	2	1	0.987482	Class 1	AVVAEY <sup>PFSPGPPGTPKWHATK</sup> STMVWSW
S22466	A2ASS6	-0.68697	0.37929	3	1	0.971535	Class 1	NPVLMKDVAYPPGPPS <sup>NAHVTD</sup> TTKKSASLA
S15406	A2ASS6	-0.717398	0.426932	2	1	1	Class 1	NSIFL <sup>TWDPKNDGG</sup> SRIKGYIVEK <sup>CP</sup> RGSD
S24060	A2ASS6	-0.726107	0.454637	2	1	0.965865	Class 1	DSV <sup>TLSWEPPKYDGGSSINNYIVEK</sup> RDTSTT
S17508	A2ASS6	-0.743691	0.827831	3	1	0.854636	Class 1	PPGPP <sup>SCPEVKDKTKSSISLAWK</sup> PPAKDGGG
S22646	A2ASS6	-0.746741	0	3	1	0.999997	Class 1	TGKFV <sup>MTIENPAGKKSGFNVR</sup> VLDT <sup>PG</sup> PVL
Y21461	A2ASS6	-0.750766	0	2	1	0.997236	Class 1	NTEY <sup>QFRVYAVNKIGYSDPSD</sup> VPDK <sup>HCP</sup> KDI
S34464	A2ASS6	-0.758656	0.611225	2	1	1	Class 1	VTSP <sup>PRVKSPEPRVKSPETVKS</sup> PKRVK <sup>SP</sup> EP
S19128	A2ASS6	-0.761375	0.661405	3	1	1	Class 1	DSCYL <sup>TWKEPLDDGGSVW</sup> TNYV <sup>VERK</sup> DVATA
S17509	A2ASS6	-0.765849	0.574468	2	1	0.499998	Class 2	PGPP <sup>SCPEVKDKTKSSISLAWK</sup> PPAKDGGG <sup>SP</sup>
S34009	A2ASS6	-0.77042	0.791858	2	1	1	Class 1	LLRPV <sup>TTTQRLSEYKSEL</sup> DYMS <sup>KEEKSK</sup> KKKS
S30820	A2ASS6	-0.787034	0	3	1	0.779125	Class 1	VLA <sup>KNAAGVISKGSESTGP</sup> VT <sup>CR</sup> DEY <sup>AP</sup> PKA
S34653	A2ASS6	-0.82199	0.752192	2	1	0.95726	Class 1	SSKPV <sup>VITGLRDTTVSSDS</sup> VAK <sup>FTIK</sup> VTGEP
S32936	A2ASS6	-0.824822	0	3	1	0.909829	Class 1	DVSR <sup>DSVNLWTEPASDGGSKVTNYIVEK</sup> CA
T16910	A2ASS6	-0.831267	0.77835	3	1	1	Class 1	LDVSV <sup>KGGIQIMAGKTLRIPAE</sup> VTGR <sup>P</sup> VPTK
S15236	A2ASS6	-0.836399	0.546251	3	1	0.997816	Class 1	DQV <sup>LEEGDRVKMKTISAYAE</sup> LVIS <sup>P</sup> SERTDK
S21637	A2ASS6	-0.851016	0.751694	2	1	0.999673	Class 1	WSTV <sup>TTECSKTSFRVSN</sup> LEEG <sup>KSYFFRV</sup> FAE
T30103	A2ASS6	-0.851493	0	3	1	0.499919	Class 2	DWHK <sup>VNTEPCVKTRYTVTDL</sup> QAGEEY <sup>K</sup> FRVS
S32230	A2ASS6	-0.864269	0.82444	2	1	0.991873	Class 1	DPFD <sup>KPSQPGELEILSISK</sup> SV <sup>LQ</sup> WEK <sup>PE</sup> C
S34005	A2ASS6	-0.876525	0	3	1	0.999798	Class 1	EEEE <sup>LLRPVTTTQRLSEYKSEL</sup> DYMS <sup>KEEKS</sup>
S18731	A2ASS6	-0.87685	0.25695	3	1	0.995523	Class 1	EY <sup>MVISWKPPLDDGGSEITNYIEK</sup> ELG <sup>KD</sup>
S4248	A2ASS6-3	-0.893375	0	4	1	0.967119	Class 1	VQGE <sup>PVRTHFYDHTVSPFA</sup> AQSN <sup>I</sup> KEY <sup>TIRE</sup>
T30453	A2ASS6	-0.895531	0.674399	3	1	0.861201	Class 1	LTGIT <sup>NQLITCKAGSTFTID</sup> VPIS <sup>GR</sup> PAP <sup>KV</sup>
S1805	A2ASS6	-0.895653	0.717555	2	1	1	Class 1	GTD <sup>HTSATLVKDEKSLV</sup> ESQL <sup>PDG</sup> GKGL <sup>Q</sup>
S15266	A2ASS6	-0.907094	0	2	1	0.977731	Class 1	KGIY <sup>TLTLENPVKSISGEIN</sup> VNIAPP <sup>S</sup> APK
S25399	A2ASS6	-0.923229	0.531448	2	1	0.967678	Class 1	VIA <sup>KNAAGAIKPSDSTG</sup> PNITAK <sup>DE</sup> VEL <sup>PR</sup> I
S27960	A2ASS6	-0.925189	0.489628	2	1	0.834475	Class 1	RVR <sup>SLNKM</sup> GASDP <sup>SDSDPQ</sup> VAKERE <sup>EE</sup> EPV <sup>F</sup>
S3286	A2ASS6	-0.938293	0.866542	2	1	0.851679	Class 1	RPQ <sup>PKISWYKEEQ</sup> LLST <sup>GF</sup> KCK <sup>FL</sup> H <sup>DG</sup> QEY <sup>T</sup>
T22529	A2ASS6	-0.943427	0.67514	2	1	1	Class 1	GTAL <sup>RITQFVW</sup> PD <sup>LQ</sup> TKE <sup>YN</sup> FRISA <sup>IND</sup> AG
S4720	A2ASS6-3	-0.959846	0	3	1	0.9499	Class 1	PRGA <sup>VHGAEPHRR</sup> LSL <sup>SQDL</sup> PFL <sup>MT</sup> G <sup>EQD</sup>
S35060	A2ASS6	-0.967557	0	2	1	0.845469	Class 1	SASK <sup>QEASFSSSSS</sup> ASSM <sup>TEMK</sup> FAS <sup>MS</sup> SA <sup>Q</sup>
Y20757	A2ASS6	-0.96841	0.688841	2	1	0.999745	Class 1	SSV <sup>LI</sup> KDV <sup>TRKDSG</sup> YSL <sup>TAENS</sup> SGSD <sup>T</sup> Q <sup>K</sup>
S25797	A2ASS6	-0.975471	0.492227	2	1	0.999986	Class 1	IRV <sup>CALNKVGLG</sup> EAAS <sup>VP</sup> GT <sup>VK</sup> PE <sup>D</sup> KLEA <sup>PE</sup>
S23925	A2ASS6	-1.00025	0.887458	3	1	0.999906	Class 1	VSA <sup>QNEK</sup> GISD <sup>PRQL</sup> SV <sup>PIAKDL</sup> V <sup>IP</sup> PA <sup>FK</sup>
S25613	A2ASS6	-1.02282	0.946511	2	1	1	Class 1	PVLM <sup>KNPFVLP</sup> GP <sup>PKS</sup> LE <sup>V</sup> TNIA <sup>KDS</sup> M <sup>T</sup> VC <sup>W</sup>
S29299	A2ASS6	-1.03903	0.614927	2	1	0.999999	Class 1	TDYL <sup>VERK</sup> GK <sup>GEQAW</sup> SHAGIS <sup>KT</sup> CEI <sup>E</sup> IG <sup>QL</sup>
Y20182	A2ASS6	-1.04142	0.707871	3	1	1	Class 1	TGP <sup>P</sup> TES <sup>K</sup> PIA <sup>KTYDRP</sup> GR <sup>PD</sup> PE <sup>V</sup> TK <sup>V</sup> S
S35104	A2ASS6	-1.0585	0	2	1	0.746582	Class 2	SSS <sup>FMGKSSMTQLES</sup> STR <sup>MLK</sup> AG <sup>GR</sup> G <sup>IP</sup> PK
S15616	A2ASS6	-1.06363	0.707178	2	1	0.999998	Class 1	GSK <sup>ITNY</sup> VER <sup>KATDSD</sup> V <sup>WHKLS</sup> ST <sup>V</sup> K <sup>D</sup> T <sup>NF</sup>
S20732	A2ASS6	-1.08258	0.581344	2	1	0.997277	Class 1	PICK <sup>WK</sup> GD <sup>DEW</sup> TSS <sup>HLAIH</sup> KAD <sup>G</sup> SS <sup>V</sup> L <sup>II</sup>
T16946	A2ASS6	-1.0848	0	2	1	1	Class 1	EGEL <sup>D</sup> KER <sup>VIEN</sup> VG <sup>TKSE</sup> LI <sup>KNAL</sup> R <sup>KD</sup> H <sup>G</sup>
S24436	A2ASS6	-1.0957	0.769352	3	1	0.997797	Class 1	KVLD <sup>RP</sup> GP <sup>PE</sup> GP <sup>VAIS</sup> GV <sup>TAEK</sup> CT <sup>LAWK</sup> PL
S19776	A2ASS6	-1.13133	0	4	1	0.570984	Class 2	VRAD <sup>H</sup> G <sup>KY</sup> ISAK <sup>NSSG</sup> H <sup>AQGS</sup> AIN <sup>V</sup> LD <sup>RP</sup>
T30100	A2ASS6	-1.14081	0.86237	2	1	0.999845	Class 1	DLGD <sup>WHKVNTEPCVKTRYTVTDL</sup> QAGEEY <sup>K</sup> F

(Continued)

TABLE 3 | Continued

Position within titin	UniProt identifier	Log2 ratio (KO/WT)	−Log 10 p-value KO/WT	Charge	Multiplicity	Localization probability	Classification of phosphosite	Sequence window
S28970	A2ASS6	−1.14229	0.390143	2	1	0.848484	Class 1	PPGPPAKIRIADSTKSSITLGWSKPVYDGGG
S23728	A2ASS6	−1.15678	0	2	1	0.680757	Class 2	FDSGKYILTVENSSGSKSAFVNVRVLDTPGP
S23604	A2ASS6	−1.18392	0	2	1	0.760984	Class 1	DEWQVWTPPAGLKATSYTITSLIENQEYKIR
T22805	A2ASS6	−1.18392	0.725798	2	1	0.948992	Class 1	IEAQRKGSQDQWTHISTVKGLECVRNLTGE
S25730	A2ASS6	−1.2141	1.02176	2	1	0.999999	Class 1	AHVVDTTKNSITLAWSKPIYDGGSEILGYV
S24155	A2ASS6	−1.21435	0.495954	3	1	0.938049	Class 1	LASKDSMEVQWHEPVSDDGGSKVIGYHLERKE
T23603	A2ASS6	−1.22489	0.565233	2	1	0.891141	Class 1	EDEWQVWTPPAGLKATSYTITSLIENQEYKI
S29402	A2ASS6	−1.22605	1.20053	2	1	1	Class 1	LKDGLPLKESEYVRFSSKTENKITLSIKNSKK
T25518	A2ASS6	−1.23095	0.735191	3	1	0.981598	Class 1	KVLDLDRPGPEGPVQVTGVTAEKCTLAWSPPL
T19879	A2ASS6	−1.23865	1.098	3	1	1	Class 1	CAENKVGVGPTIETKTPILAINPIDRPGPEPE
Y29398	A2ASS6	−1.26528	0.758789	2	1	1	Class 1	SISWLKDGGLPLKESEYVRFSSKTENKITLSIK
S32140	A2ASS6	−1.27419	0.799964	2	1	0.998818	Class 1	PEVLDVTKSSVLSWSRPPKDDGGSRVTGYI
S28985	A2ASS6	−1.28346	0	2	1	0.999999	Class 1	SSITLGWSKPVYDGGSDVTGYVEMKQGDDEE
S35029	A2ASS6	−1.33441	0	3	1	0.960754	Class 1	PLVEEPPREWLTSSDVSLLHGSVSSQSVQM
S34457	A2ASS6	−1.40297	0	2	2	1	Class 1	ARVIEKAVTSPPRVKSEPEPRVKSPETVKSPPK
S35096	A2ASS6	−1.44254	0.872837	2	1	0.869587	Class 1	QESFVEMSSSSFMGKSSMTQLESSTSRMLKA
T22515	A2ASS6	−1.45339	0	3	1	0.998937	Class 1	HQKVGDDAWIKDITGTALRITQFVWPDQLTK
S25026	A2ASS6	−1.48484	0.743171	3	1	0.949735	Class 1	IAKDLVIEPDRPAFSSYSVQVGGDLKIEVP
S21724	A2ASS6	−1.49957	0	2	1	0.965611	Class 1	VDFLTEENKWRVMKSLSLQYSTKDLKEGKE
S27185	A2ASS6	−1.55785	0.714422	2	1	1	Class 1	QLGVPVIAKDIEIKPSVELPFNTFNKANDQ
S34009	A2ASS6	−2.60171	0	2	2	1	Class 1	LLRPVTTTQRLSEYKSELDYMSKEEKSKKKS

Novex-3 (A2ASS6-3).

Z-disk.

Proximal Ig region.

Middle Ig region.

A-band.

M-band.

(ELISA). Hydrogen peroxide (H<sub>2</sub>O<sub>2</sub>) was assessed in LV tissue homogenates ( $n = 4$ –10/group). Samples containing equal amounts of total protein were analyzed for H<sub>2</sub>O<sub>2</sub> formation. Total reduced glutathione in heart samples was determined in duplicate with a colorimetric glutathione assay kit (CS0260, Sigma Aldrich).

## Amount and Phosphorylation of PKD and HSP27

The content of PKD and HSP27, as well as their phosphorylation were measured by 15% SDS–PAGE and western blot.

## CaMKII Content and Activity

The content of CaMKII was determined using 15% SDS–PAGE and western blot and its activity by using non-radioactive kinase activity-assay kit (CycLex).

## Immunofluorescence Imaging

Frozen histological LV sections ( $n = 3$ /group) were fixed, blocked and dual-stained with anti-PKD (Sigma-Aldrich; dilution 1:200) or anti-phospho-HSP27 (Ser 82) (Cell Signaling Technology; 1:50) and anti- $\alpha$ -actinin (sarcomere; Sigma-Aldrich; dilution 1:400) antibody, and were incubated with

the appropriate secondary antibodies: (FITC) anti-mouse (Rockland Immunochemicals Inc, Limerick, PA, USA; dilution 1:300) and Cy3 anti-rabbit (Jackson ImmunoResearch Laboratories Inc, West Grove, PA, USA; dilution 1:100). Immunostained samples were analyzed by confocal laser scanning microscopy (Nikon Eclipse Ti-E Inverted Microscope System; Nikon Instruments, Nikon Corp, Shinagawa, Tokyo, Japan). Immunofluorescence imaging was processed equally among groups, for 2D intensity histogram analysis the Coloc2 plugin in FIJI was used.

## Electron Microscopy (EM)

Frozen LV samples were cut, fixed and blocked. Samples were then immunolabeled against primary antibodies of PKD (Abcam; 1:200) and HSP27 (Abcam; 1:200), then with nanogold conjugated secondary antibodies. After counterstaining with osmium-tetroxide, and dehydration, blocks were embedded into resin. 50 nm thin sections were cut.

## Statistics

Values are given as mean  $\pm$  SEM. Statistically significant differences were tested using Bonferroni adjusted unpaired or paired Student's  $t$ -test, with  $P < 0.05$  considered significant.

**TABLE 4** | Upregulated titin phosphosites (log<sub>2</sub> ratio KO/WT > 0.37).

Position within titin	UniProt identifier	Log <sub>2</sub> ratio (KO/WT)	−Log <sub>10</sub> p-value KO/WT	Charge	Multiplicity	Localization probability	Classification of phosphosite	Sequence window
T314	A2ASS6	0.386936	1.09573	2	1	0.982868	Class 1	TPSPVRSVSPAGRISTSPIRSVKSPLLIRKT
T10276	A2ASS6	0.395205	0	3	1	0.637793	Class 2	EVQKKVTEEKIAITQREESPPPAVPEIPK
S315	A2ASS6	0.40279	1.45166	2	1	0.997856	Class 1	PSPVRSVSPAGRISTSPIRSVKSPLLIRKTQ
S264	A2ASS6	0.419615	1.33152	2	2	1	Class 1	PHKTPPRIPPKPKRSRPTPPSIAAKAQLARQ
S35038	A2ASS6	0.429709	0.499475	2	1	0.987556	Class 1	WLKTSDDVSLHGSVSSQSVQMSASKQEASF
S262	A2ASS6	0.433659	0.711028	2	2	1	Class 1	QLPHKTPPRIPPKPKRSRPTPPSIAAKAQLA
S23788	A2ASS6	0.438542	0	2	1	0.993369	Class 1	KNYVEKRESTRKAYSTVATNCHKTSWKVDQ
S1527	A2ASS6	0.44247	0	3	1	0.86319	Class 1	VIKEDGTQSLIIVPASPSDSDGEWTVWAQNRA
S31025	A2ASS6	0.474799	0	3	1	0.838063	Class 1	GLGVPVSEPIVARNSTFTIPSQGPPEEVEGA
S834	A2ASS6	0.503759	0.543576	2	1	0.99992	Class 1	VSKISVPKTEHGYEASIAGSAIATLQKELSA
S307	A2ASS6	0.509144	3.60898	2	2	1	Class 1	VRHVRAPTPSVRSVSPAGRISTSPIRSVKS
T314	A2ASS6	0.608677	0	2	2	0.982868	Class 1	TPSPVRSVSPAGRISTSPIRSVKSPLLIRKT
S774	A2ASS6	0.620881	0.40983	2	1	0.98142	Class 1	HVVPQAVKPAVIQAPSETHIKTTDQMGMHIS
S879	A2ASS6	0.704194	0	3	2	0.998042	Class 1	TVKPGETRVRAEPTSPQFPFADMPDPDPTK
S10281	A2ASS6	0.719508	0.777963	3	1	0.999995	Class 1	VVTEEKIAITQREESPPPAVPEIPKPKVPE
S262	A2ASS6	0.720452	2.29218	2	3	1	Class 1	QLPHKTPPRIPPKPKRSRPTPPSIAAKAQLA
S264	A2ASS6	0.767076	2.14935	2	3	1	Class 1	PHKTPPRIPPKPKRSRPTPPSIAAKAQLARQ
T266	A2ASS6	0.767076	2.14935	2	3	1	Class 1	KTPPRIPPKPKRSRPTPPSIAAKAQLARQQS
S799	A2ASS6	0.787488	0	3	1	0.834492	Class 1	MGMHISSQVKKTTDISTERLVHVDKRPRTAS
S12871	A2ASS6	0.829341	1.09019	3	1	1	Class 1	AKPKGPIKGVAKKTPSPIEAERKLRPGSGG
S12884	A2ASS6	0.94305	0.52056	3	1	1	Class 1	TPSPIEAERKLRPGSGGKEPPDEAPFTYQL
S12871	A2ASS6	0.981417	0.3495	3	2	1	Class 1	AKPKGPIKGVAKKTPSPIEAERKLRPGSGG
T12869	A2ASS6	0.981417	0.3495	3	2	1	Class 1	EAAKPKGPIKGVAKKTPSPIEAERKLRPGS
S838	A2ASS6	1.20302	0	3	1	0.999952	Class 1	SVPKTEHGYEASIAGSAIATLQKELSATSSST
S32133	A2ASS6	1.4809	0.355789	2	1	0.791719	Class 1	PEPPSNPPEVLDVTKSSVLSWSRPKDDGGS

**Z-disk.****PEVK.****A-band.****M-band.**

## RESULTS

We hypothesized that *Prkd1* cKO mouse hearts would show altered titin phosphorylation compared to matched WT hearts.

### Quantitative Mass Spectrometry Detects Disturbed Regulation in *Prkd1* cKO Mice

Using the SILAC technique, we detected a wide range of cardiac proteins that were either significantly upregulated (>80 proteins), downregulated (>105 proteins) or unchanged (remainder) in cKOs (Figure 1A). In total we detected 9,833 phosphosites (4,859 of them with  $-\log_{10} p > 0$ ) from 3,652 different proteins (2,507 of them with  $\log_{10} p > 0$ ) (Figure 1B). In total, 505 proteins were downregulated in cKO ( $\log_2$  ratio KO/WT < −0.37) with a significant downregulation of 105 proteins. In addition to 422 proteins found to be upregulated ( $\log_2$  ratio KO/WT > 0.37), 80 proteins showed a significant upregulation, while the rest remained either unchanged or with no relevant pvalue (Figure 1A). Among the significantly up- or downregulated proteins were numerous myofibrillar and calcium handling proteins, in addition to several phosphatases and kinases (Figures 1C–F). We also detected

many cardiac peptides that were either hypophosphorylated (70 phosphopeptides), hyperphosphorylated (63 phosphopeptides), or unchanged in cKOs (Figure 1B).

### Quantitative Mass Spectrometry Detects Conserved PKD Phosphosites in Titin

Quantitative MS was combined with a modified SILAC technique to facilitate identification of PKD-dependent phosphorylation sites in titin. Titin was among the proteins that showed the largest alterations in phosphorylation in cKO compared to WT hearts. We identified 332 titin phosphopeptide (including 77.7% serines, 19.3% threonines, and 3.0% tyrosines), including 258 phosphosites with a ratio of cKO to WT phosphorylation levels (ratio WT/cKO) for titin. Among them, 164 phosphosites were with  $-\log_{10} p > 0$  (Figure 2A). Most of the identified phosphopeptides were class 1 (localization probability 0.75–1.00), although 27 phosphopeptides showed a localization probability < 0.75 and were therefore class 2 phosphopeptides (see Tables 1–5). The majority of the phosphopeptides showed single phosphorylation, although some showed double phosphorylation. According to the conservative estimate that a cKO/WT ratio should be  $\leq -0.37$  or  $\geq +0.37$  in order to

**TABLE 5** | Unchanged titin phosphosites ( $-0.37 < \log_2 \text{ratio KO/WT} < 0.37$ ).

Position within titin	UniProt identifier	Log <sub>2</sub> ratio (KO/WT)	-Log <sub>10</sub> p-value KO/WT	Charge	Multiplicity	Localization probability	Classification of phosphosite	Sequence window
T26299	A2ASS6	-0.367305	0.338896	2	1	0.999988	Class 1	PVVQYPFKEPGPPGTPFVTSISKDQMLVQW
S23354	A2ASS6	-0.359797	0	3	1	0.990613	Class 1	KVLDRPGPEGLAVSDVTSEKCVLSWLPL
S34298	A2ASS6	-0.356955	0	3	1	0.609727	Class 2	YAVSSFKRTSELEAASSVREVKQMTETRES
S34470	A2ASS6	-0.355278	0	2	1	1	Class 1	VKSPEPRVKSPETVKSPPKRVKSPEPVTSHPK
S33875	A2ASS6	-0.353589	0.477593	3	2	1	Class 1	PSPDYDLYYYRRRRRSLGDMSEDELLLPIDD
S33880	A2ASS6	-0.353589	0.477593	3	2	1	Class 1	DLYYYRRRRRSLGDMSEDELLLPIDDYLAMK
S18562	A2ASS6	-0.350673	0.345871	2	1	1	Class 1	IGTEKFHKVTNDNLLSRKYTVKGLKEGDTYE
T22520	A2ASS6	-0.329784	0	3	1	0.995336	Class 1	DDAWIKDTTGTALRITQFVWPDLQTKKEYNF
S3977	A2ASS6	-0.319098	0.36361	2	1	0.840288	Class 1	CTEGKILMASADTLKSTGQDVALRTEEGKSL
S19146	A2ASS6	-0.318534	0.168528	2	1	0.995484	Class 1	TNYVVERKDVATAQWSPSLSTTSKKKSHMAKH
T13665	A2ASS6	-0.316873	0.41921	2	1	1	Class 1	CEVSREPKTFRWLKGTQEITGDDRFELIKDG
S17098	A2ASS6	-0.305806	0.472482	2	1	0.933227	Class 1	PPTSPERLTYTERTKSTITLDWKEPRSDGGS
S24868	A2ASS6	-0.302999	0	2	1	0.998408	Class 1	KIKNYIVEKREATRKSYYAAVNTNCHKNSWKI
S34470	A2ASS6	-0.302672	0.238728	2	2	1	Class 1	VKSPEPRVKSPETVKSPPKRVKSPEPVTSHPK
S26806	A2ASS6	-0.301597	0	2	1	0.655766	Class 2	PPGPPSNPKVTDTSRSSVSLAWNKPIYDGGGA
S18224	A2ASS6	-0.300622	0.391952	2	1	0.832005	Class 1	APPGPPFPKVDWTKSSVDLEWSPPLKDGGS
S34464	A2ASS6	-0.2992	0.235518	2	2	1	Class 1	VTSPPRVKSPETVKSPPKRVKSPEP
S2080	A2ASS6	-0.298846	0.520376	2	1	1	Class 1	ITPTFKPERIELSPSMEAPKIFERIQSQT
S19448	A2ASS6	-0.273899	0	2	1	0.805061	Class 1	QDTRKGTWGVVSAGSSKLLKVPHLQKGCYE
S13228	A2ASS6	-0.273069	0	2	1	0.993076	Class 1	DIPGEWKLKCELLRPSPTCEIKAEKGRFLT
S27374	A2ASS6	-0.266139	0	3	1	0.820467	Class 1	SSYSESSAWAEYFPSPGPPGTPKVVHATK
S20517	A2ASS6	-0.265893	0	3	1	0.748614	Class 2	TSCHVSWAPPENDGGSQVTHYIVEKREARERK
S28343	A2ASS6	-0.263658	0	3	1	0.780076	Class 1	SVTTDAGRYEITAANSSGTTKFINIIVLDR
S32318	A2ASS6	-0.262435	0.516907	2	1	0.999971	Class 1	SRPRRTAMSVKTKLTSGEAPGVRKEMADVTT
S3622	A2ASS6-3	-0.260512	0	3	1	0.962608	Class 1	VEEKGMVRTIHFRRASPVRRADYVYNDWSE
Y21274	A2ASS6	-0.257528	0	3	1	1	Class 1	VGDPILTEPAIAKNPYDPPGRCDPPVISNIT
T22220	A2ASS6	-0.252516	0.8886	3	1	0.940036	Class 1	AGKDIRPSDIAQITSTPTSSMLTVKYATRKD
S22152	A2ASS6	-0.241103	0	2	1	0.761358	Class 1	IRAKNTAGAISAPSESTGTIICKDEYEAPTI
S20332	A2ASS6	-0.239112	1.58029	2	1	1	Class 1	IIGYVEMRPKIADASPDDEGWKRCNAAQLI
S9201	A2ASS6	-0.230981	0	2	1	1	Class 1	IMFKNNALLQVKRASPMADAGLYTCKATNDA
S4098	A2ASS6-3	-0.229673	0	3	1	1	Class 1	FELPEVTPRDQAIQSPKHKFISSDITNEP
S27782	A2ASS6	-0.229019	0	3	1	0.547507	Class 2	DPFTTSPPTSLEITSVTKDSMTLWVSRPET
T27228	A2ASS6	-0.228542	0.209869	3	1	0.955571	Class 1	ATVAWKKDGQVLRRETRRVNVAASKVTVTL
S20036	A2ASS6	-0.211545	0	2	1	0.999133	Class 1	EVAWTKDKDADLDRSPRVKIDTSAESSKFS
S9144	A2ASS6	-0.203903	0.163212	2	1	1	Class 1	NIKERLIPPSFTKLSSETVEETEGNSFKLEG
S22416	A2ASS6	-0.192457	0	2	1	0.999998	Class 1	EKKGLRWVRATKTPVSDLRCKVTLGLEQNTY
S30939	A2ASS6	-0.186488	0	2	1	0.998923	Class 1	VKVLDSPGPCGKLTVSRVTEEKCTLAWSLPQ
S18535	A2ASS6	-0.184072	0	3	1	1	Class 1	NTVSLTWNPPKYDGGSEIINYVLESRLIGTE
T266	A2ASS6	-0.174257	0.297613	2	1	1	Class 1	KTPPRIPPKPSRSPTPPSIAAKAQLARQQS
S4175	A2ASS6	-0.168399	0.396358	3	1	1	Class 1	HEEDKIDVQGGRDHLSDAQKQVETVIEAEADS
T23981	A2ASS6	-0.166376	0	3	1	0.5	Class 2	PAVTWHKDDIPLKQTRVNAESTENNSLLTI
T14268	A2ASS6	-0.16409	0.087451	2	1	0.99985	Class 1	VFTKNLANLEVSEGDTIKLVCEVSKPGAIEVI
S1529	A2ASS6	-0.159512	0.439196	3	1	0.943823	Class 1	KEDGTQSLIIVPASPSDSEGEWTVVAQNRAK
S9459	A2ASS6	-0.158813	0.124587	3	1	1	Class 1	DLRAMLKKTALKKSGSEEEIIMELLKNV
T30575	A2ASS6	-0.154592	0	3	1	0.788648	Class 1	TEITNYIVEKRESGTTAWQLINSSVKRTQIK
S28281	A2ASS6	-0.146693	0.305079	3	1	0.999999	Class 1	DMKNFPSHTVYVRAGSNLKVDPISGKPLPK
S26695	A2ASS6	-0.140014	0.346765	3	1	0.797368	Class 1	EPVIACNPYKRPSPSTPEASAITKDSMVL
S24391	A2ASS6	-0.137242	0.088548	2	1	0.993652	Class 1	TARLEIKSTDFATSLSVKDAVRVDSGNYLK
T29649	A2ASS6	-0.134127	0.58377	3	1	0.997724	Class 1	PSKFTLAVSPVDPGTPDYIDVTRETTILKW

(Continued)

TABLE 5 | Continued

Position within titin	UniProt identifier	Log2 ratio (KO/WT)	-Log 10 p-value KO/WT	Charge	Multiplicity	Localization probability	Classification of phosphosite	Sequence window
T21731	A2ASS6	-0.127027	0	2	1	0.718367	Class 2	NKWQRVMKSLSLQYSTKDLKEGKEYTFRVSA
T33772	A2ASS6	-0.120166	0.177658	2	1	1	Class 1	RMPYEVPEPRRFKQATVEEDQRIKQFVPMSD
S16477	A2ASS6	-0.120059	0.290657	2	1	0.960016	Class 1	KAVDPIDAPKVLRLTSLEVKRGDEIALDATI
T25842	A2ASS6	-0.117083	0	2	1	0.999999	Class 1	AGGSARIHIPFKGRPTPEITWSKEEGFTDK
S17015	A2ASS6	-0.116476	0	3	1	0.999637	Class 1	KMCLLNWSDPADDGGSDITGFIIERKDAKMH
S3827	A2ASS6-3	-0.110284	0.69199	2	1	1	Class 1	SNEEVHGYKSRGICESPKDKVSQLTPYPSES
S34488	A2ASS6	-0.108085	0.264442	2	1	0.999994	Class 1	RVKSPEPVTSHPKAVSPTETKPTKEGQHLPV
S790	A2ASS6	-0.10482	0	3	1	0.790373	Class 1	ETHIKTTDQMGMHISSQVKTTDISTERLVH
T26696	A2ASS6	-0.0857946	0.182593	3	1	0.989467	Class 1	PVIACNPYKRPGPPTPEASAITKDSMVLTW
S1977	A2ASS6	-0.081692	0.055874	2	1	0.990373	Class 1	KLQFEVQKVRPVDTSKTEWVWKLKRAERIT
S19447	A2ASS6	-0.0663668	0	2	1	0.591546	Class 2	KQDTRKGTWGVWSAGSSKLLKLVPHLQKGCE
S13204	A2ASS6	-0.0662166	0.089154	2	1	0.880947	Class 1	LKPIEDVTIYEKESASFDAIESEEDIPGEWK
S25920	A2ASS6	-0.0488367	0.044418	3	1	1	Class 1	PGPPQNLAVKEVRKDSVLLWWEPIIDGGAK
S22804	A2ASS6	-0.0380723	0.014722	2	1	0.805129	Class 1	VIEAQRKGSQDQWTHISTVKGLECVWRNLTEG
S34611	A2ASS6	-0.0345249	0	2	1	0.68296	Class2	TGQSFKSIHEQVSSISSETTKSVQKTAESAEA
S30572	A2ASS6	-0.0335397	0	2	1	0.832922	Class 1	DGGTEITNIVYKRESGTTAWQLINSSVKRT
S35063	A2ASS6	-0.0245479	0	2	1	0.632417	Class2	KQEASFSFSSSSASSMTEMKFASMSAQSMS
S4018	A2ASS6	-0.018641	0	2	1	0.675564	Class 2	VLLKEEQSEVAVPTSQTSKSEKEPEAIKGV
S35036	A2ASS6	-0.0161605	0	2	1	0.952755	Class 1	REVLKTSDDVSLHGSVSSQSVQMSASKQEA
S3991	A2ASS6	-0.0149712	0.0107483	2	1	0.999502	Class 1	KSTGQDVALRTEEGKSLSPFLALEEKQVLLK
S17113	A2ASS6	-0.01187	0.0154739	3	1	0.985972	Class 1	STITLDWKEPRSDGGSPIQGYIIEKRRHDKP
S814	A2ASS6	-0.0108688	0.0162498	2	1	0.999999	Class 1	STERLVHVDKRPRTASPHFTVSKISVPKTEH
S20755	A2ASS6	-0.0093163	0.0181907	2	1	1	Class 1	DGSSVLIKDVTRKDSGYYSLTAENSSGSDT
S27556	A2ASS6	-0.0092088	0.0073245	2	1	0.999755	Class 1	DQRYEFRVFARNAADSVSEPESTGPITVKD
S3870	A2ASS6	-0.0051650	0.0056415	3	1	0.991661	Class 1	EPEGVFPGASSAAQVSPVTIKPLITLTAEPK
S4672	A2ASS6-3	-0.0048496	0.0087214	3	1	1	Class 1	ENGDKTFISQLKRAASEEELEDHEMEDGPT
S28731	A2ASS6	-0.0040724	0.0043022	2	1	0.974739	Class 1	LASILIKDANRLNSGSYELKLRNAMGSASAT
S17109	A2ASS6	0.00032406	0	3	1	0.836525	Class 1	ERTKSTITLDWKEPRSDGGSPIQGYIIEKRR
S14664	A2ASS6	0.0113125	0.0110327	2	1	1	Class 1	RIKEGKGYKFEKDGSIHRLIKDCRLEDEC
T21632	A2ASS6	0.0207359	0	2	1	0.819558	Class 1	AERKSWSTVTTECSKTSFRVSNLEEGKSYFF
S17316	A2ASS6	0.02154	0	3	1	0.980872	Class 1	ESCYLTWDAPLDNGGSEITHYIIDKRDASRK
S34623	A2ASS6	0.0307702	0.0977465	2	1	1	Class 1	SSISSETTKSVQKTAESPEAKKQEPIAPESIS
S756	A2ASS6	0.0341452	0.0943439	3	1	1	Class 1	HISTTKVPEQPRRPASEPHVWPQAVKPAVIQ
S34573	A2ASS6	0.0437442	0	3	1	0.978092	Class 1	SADGTYELKIHNLSESDCGEYVCEVSGEGT
S34571	A2ASS6	0.120101	0	2	1	0.99376	Class 1	HYSADGTYELKIHNLSESDCGEYVCEVSGEG
T32113	A2ASS6	0.130455	0	3	1	0.999962	Class 1	GISKPLKSEEPVIPKTPLNPPPEPPSNPPEVL
T25315	A2ASS6	0.134102	0	3	1	1	Class 1	NSECYVARDPCDPPGTPEAIVKRNEITLQW
S2078	A2ASS6	0.155502	0.903734	2	1	1	Class 1	GKITIPTFKPERIELSPSMEAPKIFERIQSQ
T21345	A2ASS6	0.156475	0.125556	3	1	0.999996	Class 1	PVIERTLKATGLQEGTEYFRVTAINKAGPG
S31438	A2ASS6	0.158509	0	2	1	0.78457	Class 1	VPLVPTKLEVVDTKSTVTLAWEKPLYDGGG
S34488	A2ASS6	0.158631	0	2	2	0.999994	Class 1	RVKSPEPVTSHPKAVSPTETKPTKEGQHLPV
S34476	A2ASS6	0.159999	0	2	2	1	Class 1	RVKSPETVKSPKRVKSPEPVTSHPKAVSPT
S35128	A2ASS6	0.165174	0.213397	2	1	0.999984	Class 1	GRGIPPKIEALPSDISIDEGKVLTVACAFTG
S315	A2ASS6	0.166903	0.183848	2	2	0.997856	Class 1	PSPVRSVSPAGRISTSPIRSVKSPLLRKTQ
S22797	A2ASS6	0.170233	0.274145	2	1	1	Class 1	GSKITGYVIEAQRKGSQDQWTHISTVKGLECV
S25870	A2ASS6	0.199285	0	2	1	1	Class 1	TDKVQIEGINFTQLSIDNCDNRNDAGKYILK
S13764	A2ASS6	0.200173	0	2	1	1	Class 1	SWFKNDQRLHTSKRVSMHDEGKTHSITFKDL
S814	A2ASS6	0.200474	0.566341	2	2	0.999999	Class 1	STERLVHVDKRPRTASPHFTVSKISVPKTEH

(Continued)

TABLE 5 | Continued

Position within titin	UniProt identifier	Log2 ratio (KO/WT)	-Log 10 p-value KO/WT	Charge	Multiplicity	Localization probability	Classification of phosphosite	Sequence window
S21152	A2ASS6	0.207222	0.196717	2	1	1	Class 1	RNLCTLELFSVNRKDSGDYTTITAENSSGSKS
S307	A2ASS6	0.21303	0.565178	2	1	1	Class 1	VRHVRAPTPSPVRSVSPAGRISTSPIRSVKS
S2078	A2ASS6	0.216232	0.446394	2	2	1	Class 1	GKITIPTFKPERIELSPSMEAPKIFERIQSQ
S2080	A2ASS6	0.216232	0.446394	2	2	1	Class 1	ITIPTFKPERIELSPSMEAPKIFERIQSQT
S33353	A2ASS6	0.219718	0.237812	3	1	1	Class 1	IRSQRGVSVAKVKVASIEIGPVSGQIMHAIG
T812	A2ASS6	0.223205	0.643762	4	2	0.999999	Class 1	DISTERLVHVDKRPRTASPHFTVSKISVPKT
Y33436	A2ASS6	0.229236	0	2	1	0.996224	Class 1	TKFDDGTYRCKVNDYGEDSSYAELFVKGVR
S264	A2ASS6	0.246749	0.784633	2	1	1	Class 1	PHKTPPRIPPKPKRSRPTPPSIAAKAQLARQ
S3676	A2ASS6	0.258327	0	4	1	0.878152	Class 1	EDMPLYTSVCYTIHSPDGSFGTIVNDPORG
S879	A2ASS6	0.26138	0.407205	3	1	0.998042	Class 1	TVKPGETRVRAEPTSPQFPFADMPPTDYK
S1214	A2ASS6	0.287447	0.235319	2	1	1	Class 1	IQEPKVGAIAPGFAYSEYEKEYEKEQALIRK
S322	A2ASS6	0.325277	3.06343	2	1	1	Class 1	SPAGRISTSPIRSVKSPILLIRKQTQTTMATG
S12678	A2ASS6	0.331543	0.65471	3	1	1	Class 1	IEKPKLKRPPRARPPSPKEDVKEKMFQLKA
T266	A2ASS6	0.332311	0.771702	2	2	1	Class 1	KTPPRIPPKPKRSRPTPPSIAAKAQLARQQS
S2032	A2ASS6	0.353204	0.75905	2	1	1	Class 1	EAITAVELKSRKDKESYEELLKTKTDELLHW

**Novex-3 (A2ASS6-3).**

Z-disk.

Proximal Ig region.

N2B-element.

Middle Ig region.

PEVK.

Distal Ig domains.

A-band.

M-band.

represent a significant change in cKO vs. WT, ten significantly altered titin phosphorylation sites could be identified in cKO hearts (Table 1). We identified 24 phosphosites in the elastic spring region of titin (see Table 2). Most of them were located in the N2B-element, PEVK region and distal Ig region. In total, hypophosphorylation ( $\log_2$  ratio cKO/WT  $< -0.37$ ) was seen in 133 titin phosphopeptides, the majority of which originated from A- and M-band titin (see Table 3). Furthermore, 25 titin phosphosites were hyperphosphorylated ( $\log_2$  ratio cKO/WT  $> 0.37$ ; Table 4). One hundred and twelve titin phosphopeptides showed no significant differences in phosphorylation in cKO compared to WT ( $-0.37 > \text{cKO/WT ratio} < +0.37$ ; see Table 5).

## Titin Isoform Composition in PKD1 cKO Mice

To study whether PKD has an influence on titin isoform composition, homogenized myocardial samples of cKO and matched WT mice were separated using SDS-PAGE, the protein bands visualized by Coomassie staining and the two cardiac titin isoforms N2BA and N2B analyzed using densitometry; a representative titin gel showing these two isoforms in WT and cKO is shown in Figure 2C. On average, titin isoform composition remained unchanged in cKO vs. WT mouse hearts. For both groups, the ratio of N2B to N2BA was  $\sim 85:15\%$  (Figure 2B). A “T2” titin degradation band was also detectable in hearts of both cKO and WT, but showed no significant change.

## Site-Specific Phosphorylation at Titin-N2Bus and Titin-PEVK

To confirm titin phosphorylation sites identified by quantitative MS and to analyse site-specific titin phosphorylation, affinity-purified anti-phosphosite-specific antibodies were generated against conserved serines of human/mouse N2Bus at Ser4010/Ser3991, Ser4062/Ser4043, and Ser4099/Ser4080, as well as human/mouse PEVK at Ser11878/Ser12742 and Ser12022/Ser12884. The PVDF staining served as a protein loading control.

Using the titin anti-phospho-antibodies we found unaltered phosphorylation at the positions Ser3991 (Figure 2C) and Ser4080 (Figure 2E) but significantly increased phosphorylation at the positions Ser4043 (Figure 2D), Ser12742 (Figure 2F), and Ser12884 (Figure 2G) in cKO compared to WT hearts. Using an anti-phospho-Ser/Thr antibody, overall-titin phosphorylation was found to be greatly decreased, by  $\approx 25\%$  on average, in cKO compared to WT hearts (Figure 2H).

## Cardiomyocyte $F_{\text{passive}}$ Is Elevated in cKO Hearts

The passive length-tension relationship of single skinned cardiomyocytes in relaxing solution was steeper in cKO than in WT hearts (Figures 3A,B). Significantly increased  $F_{\text{passive}}$  levels in cKO vs. WT cells were found at sarcomere lengths (SL) of  $2.1 \mu\text{m}$  or higher. Administering

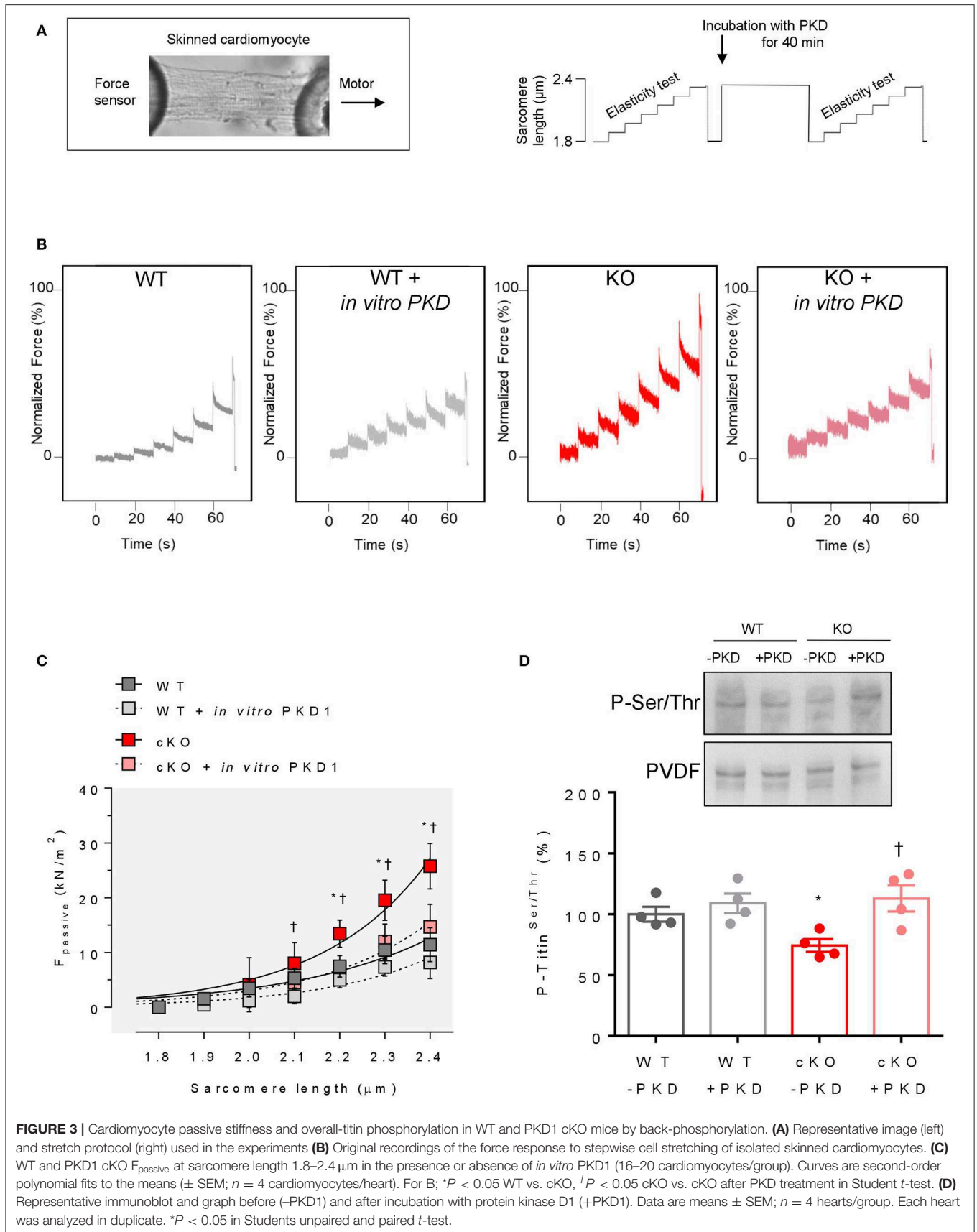
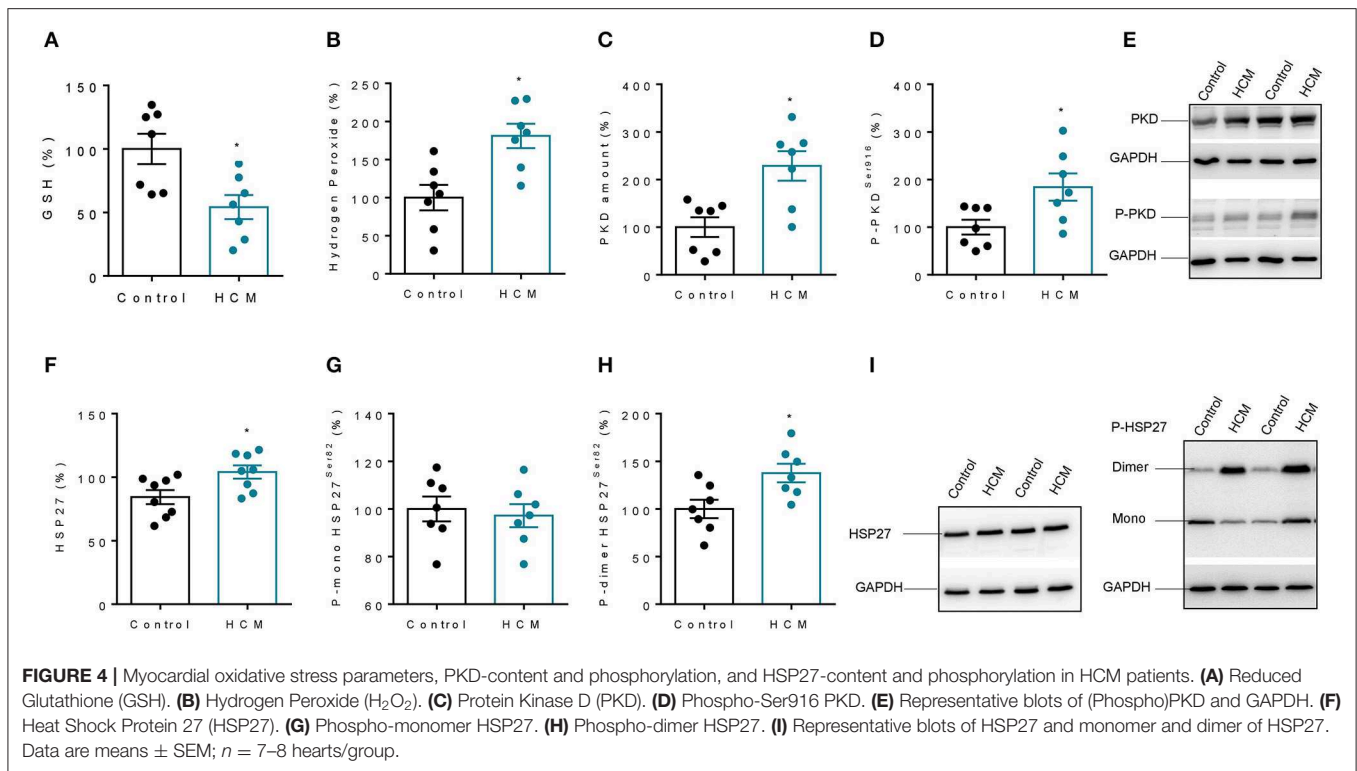


**FIGURE 3 |** Cardiomyocyte passive stiffness and overall-titin phosphorylation in WT and PKD1 cKO mice by back-phosphorylation. **(A)** Representative image (left) and stretch protocol (right) used in the experiments **(B)** Original recordings of the force response to stepwise cell stretching of isolated skinned cardiomyocytes. **(C)** WT and PKD1 cKO  $F_{passive}$  at sarcomere length 1.8–2.4 μm in the presence or absence of *in vitro* PKD1 (16–20 cardiomyocytes/group). Curves are second-order polynomial fits to the means (± SEM;  $n = 4$  cardiomyocytes/heart). For B; \* $P < 0.05$  WT vs. cKO, † $P < 0.05$  cKO vs. cKO after PKD treatment in Student *t*-test. **(D)** Representative immunoblot and graph before (–PKD1) and after incubation with protein kinase D1 (+PKD1). Data are means ± SEM;  $n = 4$  hearts/group. Each heart was analyzed in duplicate. \* $P < 0.05$  in Student's unpaired and paired *t*-test.



PKD to non-activated skinned cardiomyocytes from cKO hearts in relaxing solution significantly reduced  $F_{\text{passive}}$  at SL  $2.2 \mu\text{m}$  or higher, returning it to levels found in matched WT cells (Figure 3C), whereas administration of PKD to WT cardiomyocytes did not affect  $F_{\text{passive}}$ .

In an alternative approach, demembrated cardiac fiber bundles from hearts of these mice were phosphorylated *ex vivo* by PKD and then titin SDS-PAGE was performed followed by Western blot analysis. Titin phosphorylation was significantly increased after PKD treatment in cKO hearts, while in WT it remained unaltered (Figure 3D).

### Increased PKD and HSP27 Activity Is Associated With Increased Oxidative Stress

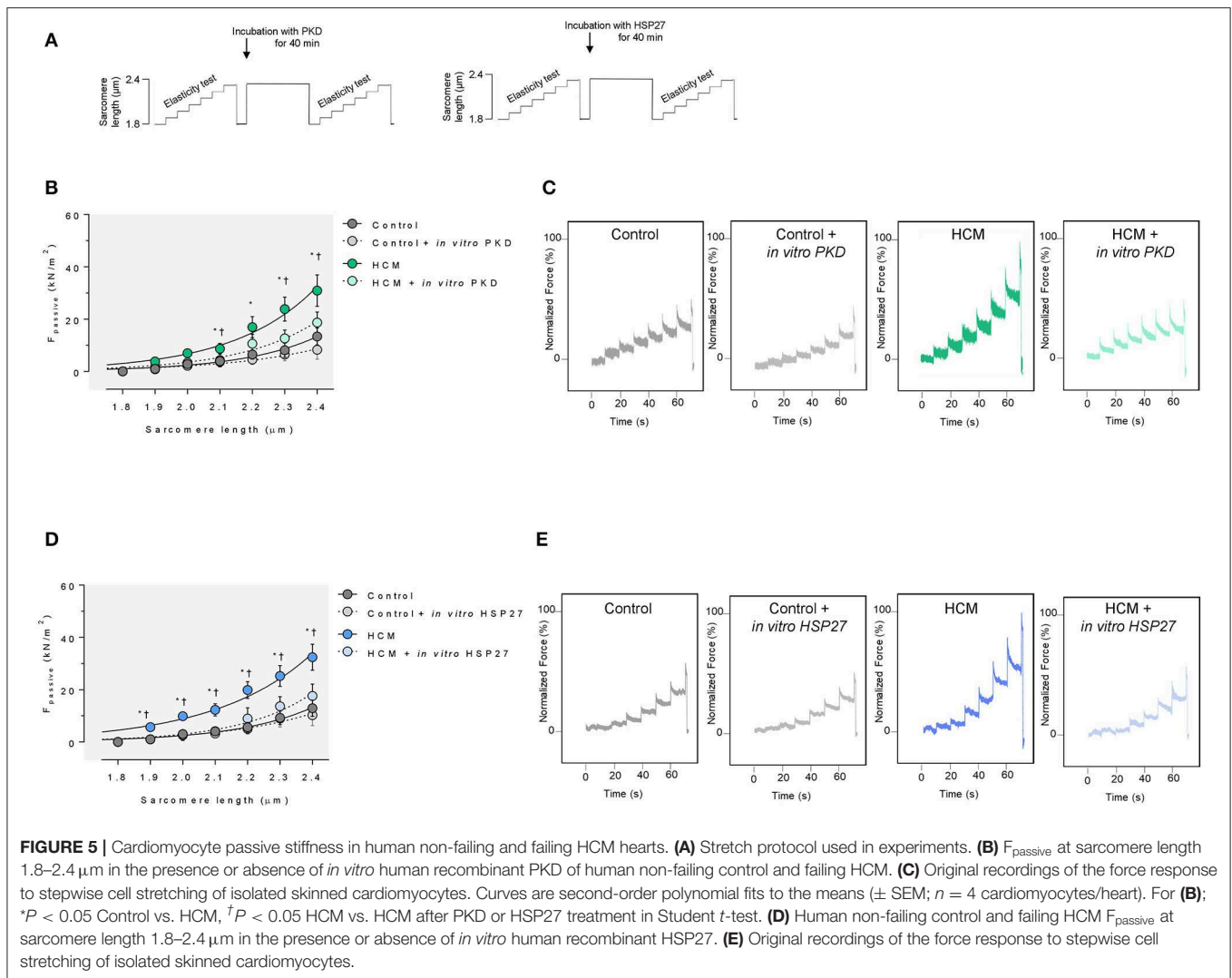
In HCM hearts, we found less reduced glutathione (GSH) and increased hydrogen peroxide ( $H_2O_2$ ), both of which indicate that oxidative stress was increased in HCM hearts compared to control non-failing hearts (Figures 4A,B). Myocardial PKD content and PKD phosphorylation at phosphosite Ser916 were both significantly higher in HCM hearts compared to controls, indicating total myocardial PKD activity in HCM (Figures 4C-E). In addition, the amount of HSP27 was higher in hearts of HCM patients compared to controls (Figure 4F) and the phosphorylation of HSP27 resulted in an altered dimer phosphorylation of HSP27 in HCM compared to controls, while HSP27 monomers remained unchanged (Figures 4G-I).

### Cardiomyocyte $F_{\text{passive}}$ Is Elevated in HCM Hearts

Cardiomyocytes from human end-stage failing hearts (only from patients with hypertrophic cardiomyopathy) showed a higher cardiomyocyte  $F_{\text{passive}}$  at sarcomere length  $2.1 \mu\text{m}$  or higher compared to non-failing human heart samples. Administering human recombinant PKD to non-activated skinned cardiomyocytes from human HCM hearts in relaxing solution significantly reduced  $F_{\text{passive}}$  at sarcomere length  $2.1 \mu\text{m}$  or higher, lowering it to levels found in cells from control hearts (Figures 5A-C). In addition, upon treatment with human recombinant HSP27,  $F_{\text{passive}}$  was significantly reduced at all sarcomere lengths, whereas control cardiomyocytes remained unaltered (Figures 5D,E).

### Titin Phosphorylation in Hearts of Human HCM Patients

We found increased CaMKII phosphosites at titin positions Ser4062 and Ser12022 in HCM compared to control hearts (Figures 6A,B), which went along with increased myocardial CaMKII content and activity (Figures 6C,D). Total titin phosphorylation was significantly lower in HCM compared to non-failing hearts (Figure 6E). Using an alternative approach, we measured total titin phosphorylation in demembrated cardiac fiber bundles obtained from HCM and non-failing human hearts before and after *ex vivo* phosphorylation by human recombinant PKD (Figure 6E). Strong signals were seen for both isoforms N2BA and N2B after kinase treatment, and the total phosphorylation of titin was significantly



increased by more than 20% in non-failing and failing HCM hearts.

### Subcellular Localization and Overlay of PKD and HSP27 in HCM and Control Hearts

As we found a relatively high level of PKD expression in failing HCM hearts using western blot, we wished to determine the cellular distribution of PKD using confocal laser scanning and electron microscopy. The confocal images showed a clear overlay of PKD signals with sarcomeres in control and HCM hearts (Figure 7A). Phospho-HSP27 was clearly present at the periphery of the cardiomyocytes in HCM compared to control hearts, whereas in control hearts, phospho-HSP27 was distributed throughout the cardiomyocyte (Figure 7B). 2D intensity histograms show two channels and the level of overlapping. For a high overlapping level, the histogram pixels tend to concentrate more along the  $y = x$  line. 2D intensity histogram analysis showed a more intense presence of PKD in HCM but distribution was not significantly different,

while phospho-HSP27 in HCM hearts compared to controls showed less correlation with  $\alpha$ -actinin as more pixels concentrate at the axis of the histogram, the less correlation can be expected (Figures 7C,D). In keeping with these findings, electron microscopy confirmed the higher level of PKD in myocardium HCM compared to control hearts (Figures 8A,B). Using electron microscopy, HSP27 showed a strongly altered localization away from the Z-disk and A-band in HCM, whereas HSP27 was located preferentially at the Z-disk and A-band in controls (Figures 8C,D).

### DISCUSSION

PKD has emerged as a key regulator of excitation-contraction coupling and cardiac hypertrophic signaling. Cardiac-specific PKD1-cKO mice show resistance to cardiac hypertrophy and fibrosis in response to pressure overload and angiotensin II treatment (Fielitz et al., 2008). Overexpression of constitutively active PKD1 in mouse hearts leads to dilated cardiomyopathy,

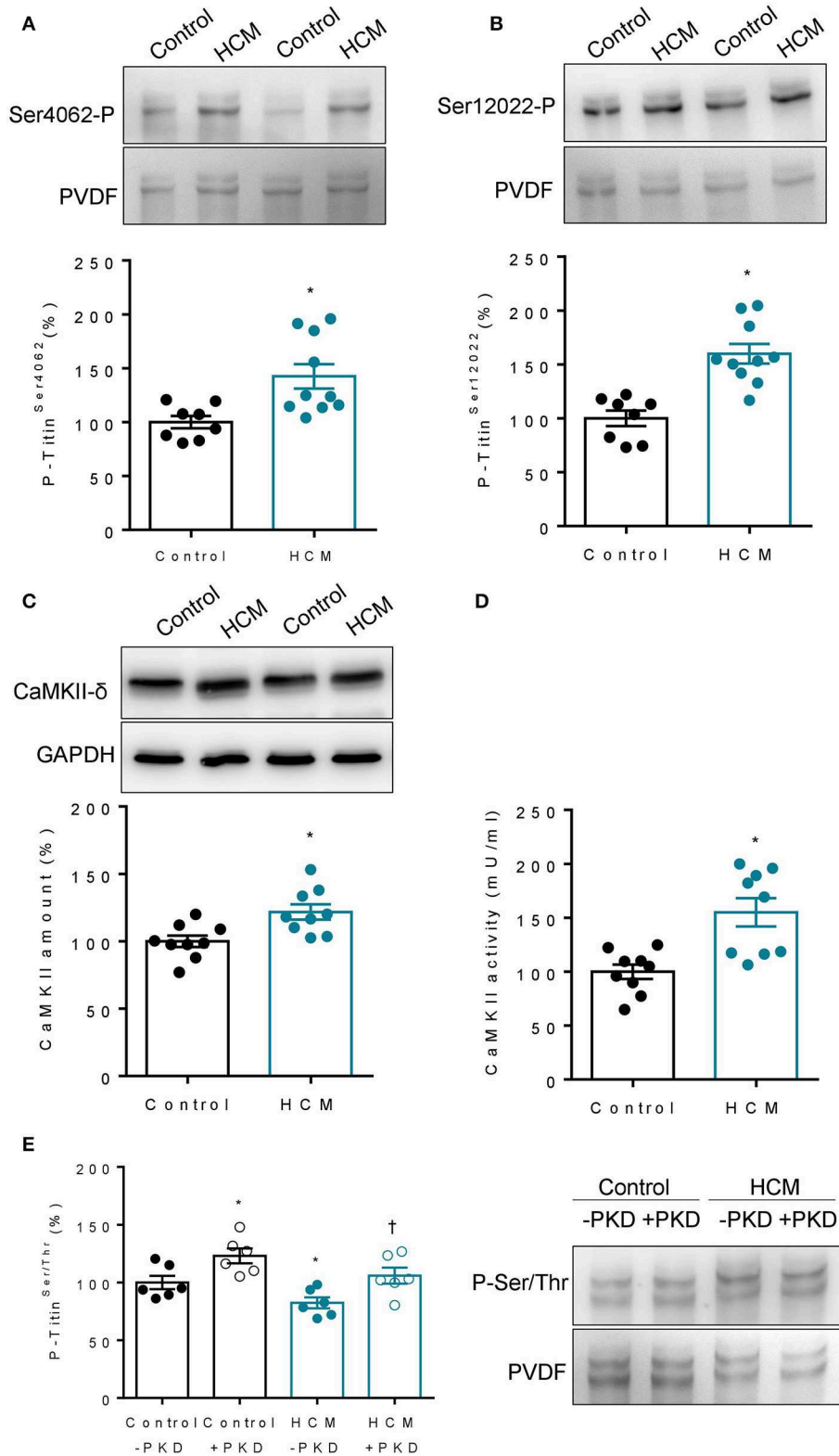


**FIGURE 6 |** Titin phosphorylation and CaMKII content and activity in hearts of failing HCM and non-failing control patients. **(A)** Site-specific phosphorylation at position Ser4062 in N2Bus ( $n = 8 - 10$  hearts/group; each heart analysed in duplicate). **(B)** Site specific phosphorylation at position Ser12022 in PEVK region ( $n = 8 - 10$  hearts/group; each heart analysed in duplicate). **(C)** CaMKII content in HCM vs. control hearts ( $n = 9$  hearts/group), or absence of *in vitro* PKD. **(D)** CaMKII  
(Continued)

**FIGURE 6** | activity in HCM vs. control hearts ( $n = 9$  hearts/group). **(E)** Total N2B-titin phosphorylation in HCM vs. control hearts ( $n = 8 - 10$  hearts/group; each heart analysed in duplicate). Representative immunoblot right panel and graph left panel before (-PKD) and after incubation with protein kinase D1 (+PKD). Data are means  $\pm$  SEM;  $n = 6$  hearts/group. Each heart was analyzed in duplicate. \* $P < 0.05$  vs. Control untreated; † $P < 0.05$  vs. HCM untreated.

and an increase in PKD1 expression and activity is seen in failing hearts of rats (Harrison et al., 2006), rabbits and humans (Bossuyt et al., 2008). These findings indicate the importance of PKD1 in regulating cardiac pathophysiology and the potential of the kinase as a therapeutic target in cardiovascular disease (Nichols et al., 2014). As PKD1 showed some beneficial effects on cardiomyocyte function (Haworth et al., 2004; Cuello et al., 2007), we wanted to know if PKD is also involved in the phosphorylation of titin. We demonstrated that titin is an important substrate of PKD. In a quantitative MS screen using PKD1-cKO hearts and the SILAC mouse heart, we found that titin was among the cardiac proteins most highly affected by PKD1 deletion. Overall, titin phosphorylation was significantly reduced in cKO compared to WT hearts. Many of the phosphosites found in titin are located within the Z-disk, A-band, or M-band sections of the molecule, where they could be involved in regulating protein-protein interactions or mechanical signaling (Figure 9). In addition, we identified many phosphosites within the I-band titin region (proximal Ig region, N2-Bus and PEVK region) present in the N2BA and N2B cardiac titin isoforms (Figure 9). Furthermore, we showed that PKD reduces cardiomyocyte stiffness in PKD1 cKO mice and in failing hearts of human HCM patients. As PKD1 activation and increased PKD1 phosphorylation is observed in the hypertrophic heart from mice that have undergone tac surgery and as PKD plays an important role in the development of cardiac hypertrophy as shown via inhibition of hypertrophy in isolated neonatal cardiomyocytes from Wistar rats with PKD deletion (Zhao et al., 2017, 2019), we used human HCM tissues to validate how important is PKD in human heart failure with hypertrophy. We found disturbed titin phosphorylation in human HCM hearts, possibly contributing to the mechanical dysfunction. This was associated with increased PKD and CaMKII content and activity in these hearts. Moreover, we detected an increased amount and phosphorylation of HSP27, a substrate of PKD, in human HCM hearts. Changes in PKD, CaMKII and HSP27 were associated with increased oxidative stress parameters. Our work reveals a previously unknown role of PKD in regulating diastolic passive properties of healthy and diseased hearts, and its association with oxidative stress and changes affecting HSP27.

## Titin Is a Substrate of PKD

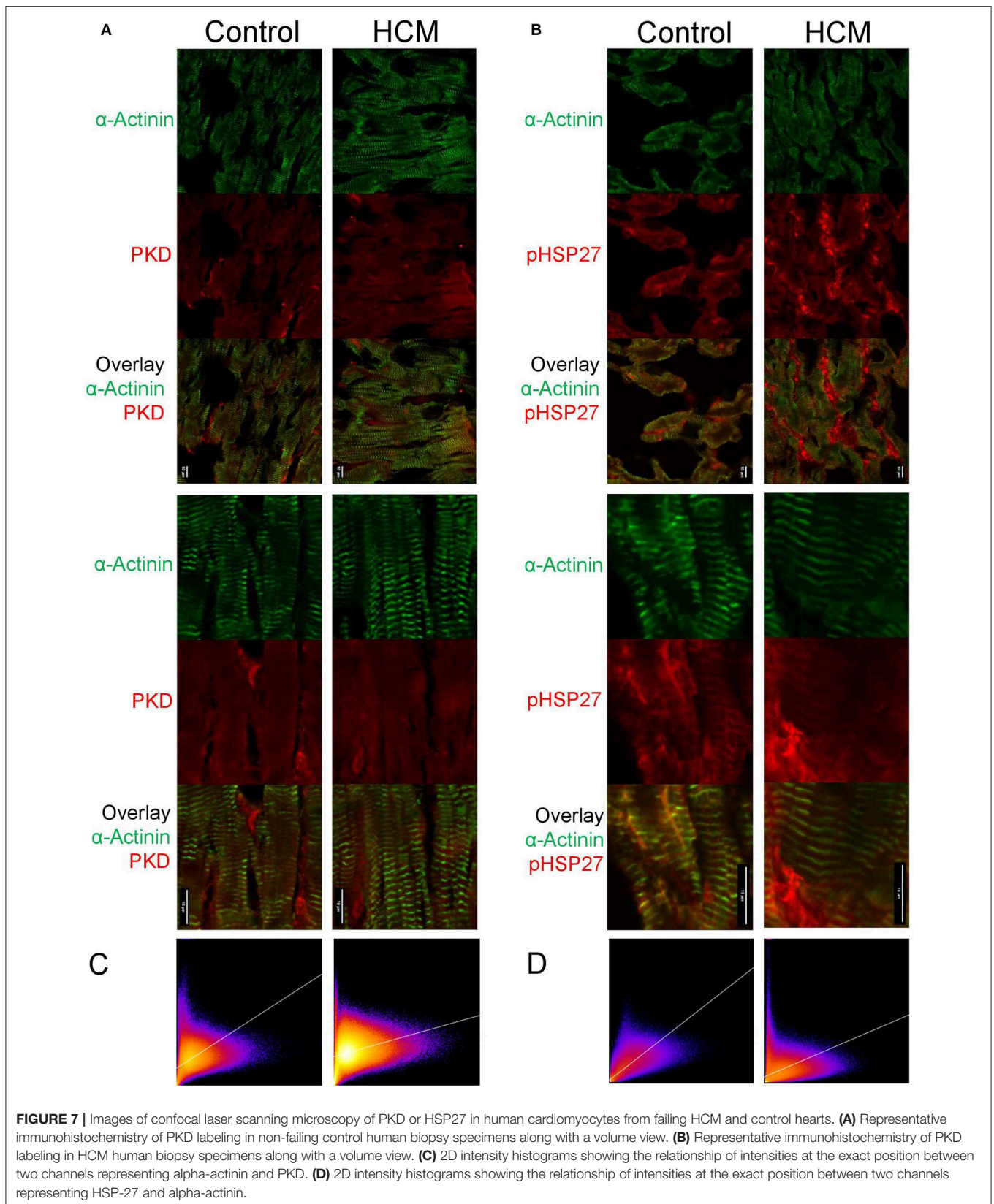
Changes in titin stiffness due to isoform switching or post-translational modifications such as phosphorylation and oxidation have been reported in a variety of species. Previous studies showed that heart failure is associated with a chronic deficit in global titin phosphorylation (Bishu et al., 2011; Falcao-Pires et al., 2011; Hamdani et al., 2013a,b). Titin is phosphorylated by PKA at the N2B spring element, which results in a reduction of cardiomyocyte  $F_{\text{passive}}$  (Yamasaki et al., 2002; Kruger and Linke, 2006). In addition, titin is phosphorylated by

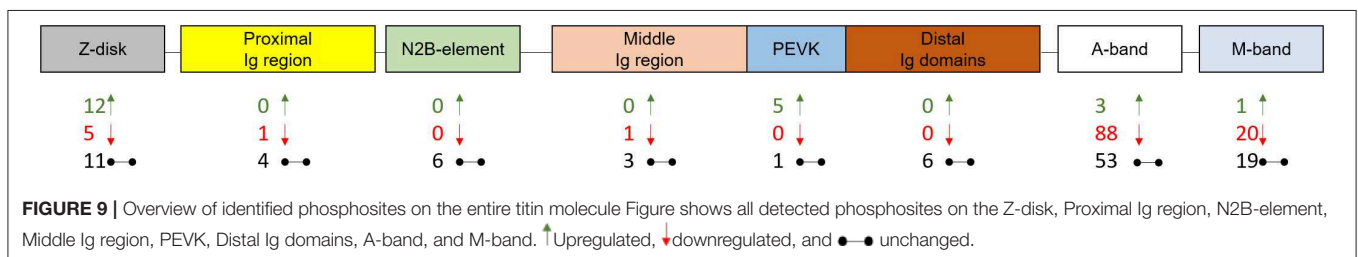
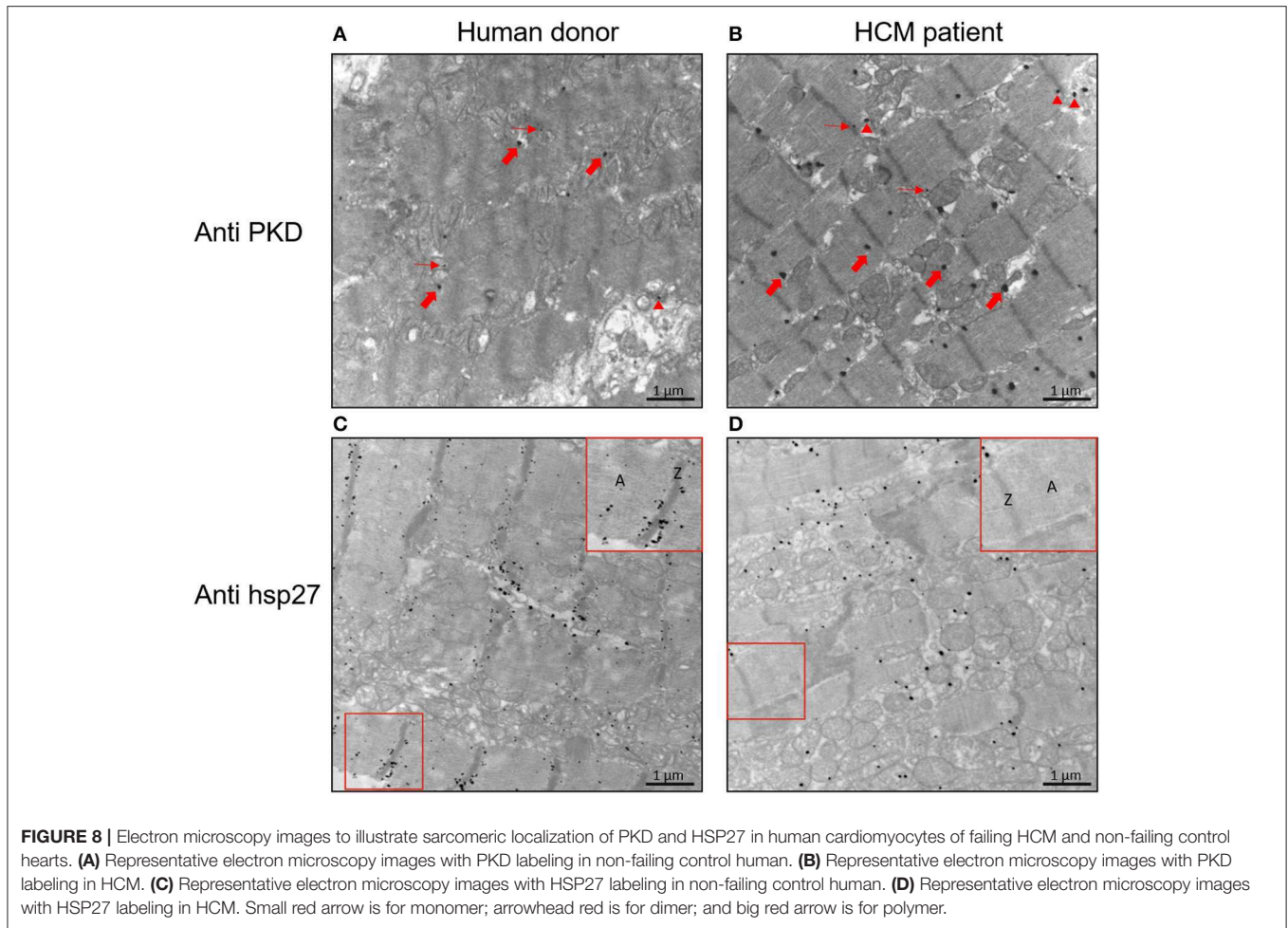
PKG at the N2Bus (Kruger et al., 2009; Kotter et al., 2013), a modification that also reduces cardiomyocyte  $F_{\text{passive}}$  (Borbely et al., 2009; Hamdani et al., 2013a, 2014). Following short-term cGMP-enhancing treatment with sildenafil and B-type natriuretic peptide (BNP) in an animal model of heart failure with preserved ejection fraction (HFpEF) (elderly hypertensive dogs) (Bishu et al., 2011), PKG-mediated phosphorylation of titin resulted in acutely increased cardiac extensibility and may also positively regulate hypertrophic signaling. Our study provides the first evidence that PKD also phosphorylates titin. Notably, altered phosphorylation of titin sites was seen within the PEVK-domain, especially at the phosphosites that are also CaMKII-dependent. Perhaps this hints at a compensatory mechanism due to the loss of PKD in these mice.

## Cardiomyocyte Stiffness and PKD

Cardiomyocyte  $F_{\text{passive}}$  was elevated in cKO compared to WT, and incubating skinned cardiomyocytes with PKD lowered  $F_{\text{passive}}$  in cKO, but did not affect WTs. Furthermore, cardiomyocyte isolated from failing HCM hearts showed increased  $F_{\text{passive}}$ , which could be reduced upon treatment with PKD enzyme. Thus, PKD alters  $F_{\text{passive}}$  in the same direction as PKA, PKG, ERK2, and CaMKII $\delta$ , an effect that may depend mainly on the phosphorylation of N2Bus. The latter increases the persistence length of N2Bus and thereby reduces  $F_{\text{passive}}$  (Kruger et al., 2009). Another possible mechanism is via phosphorylation of titin Ig domains, although this is not yet proven. To date, PKC $\alpha$  is the only kinase that increases cardiomyocyte stiffness via phosphorylation of the PEVK region. The mechanical effect of PKC $\alpha$ -mediated PEVK phosphorylation includes increased persistence length of PEVK causing increased stretch-dependent force of the titin spring, thus elevating cardiomyocyte passive tension (Hidalgo et al., 2009). Reduced all-titin phosphorylation contribute to the development of heart failure, against the reduced phosphorylation, increased phosphorylation has been demonstrated in heart failure, the PKC $\alpha$ -dependent phosphosite at S11878 within the PEVK-titin segment was hyperphosphorylated in HFpEF animal models (Hamdani et al., 2013a, 2014; Linke and Hamdani, 2014; Franssen et al., 2016). PKC $\alpha$  was shown to be increased in heart failure (Belin et al., 2007) and in the HFpEF dog hearts. We believe what might determine the spatial arrangement phosphorylation along the titin molecule is the distinct micro-environment of phospho-sites either surrounded by negatively charged micro-environment and phospho-sites located at hydrophobic environment and close to cysteines sites. This may induce distinct biological and mechanical responses that may have differential effects on heart muscle exposed to oxidative stress and inflammation.

In failing human hearts, the activities of PKA and PKG are typically reduced (Hamdani et al., 2013a, 2014; Linke and Hamdani, 2014; Franssen et al., 2016), whereas the activity





and the expression of PKC $\alpha$ , ERK2, and CaMKII $\delta$  are usually increased, perhaps because of the presence of hypertrophy. In human failing HCM hearts, cardiomyocyte  $F_{passive}$  was increased compared to non-failing hearts, an effect that was related to increased CaMKII activity and consequently, increased phosphorylation of titin within the PEVK region at CaMKII $\delta$ -dependent phosphosites (Bishu et al., 2011; Falcao-Pires et al., 2011; Hamdani et al., 2013a,b). Cardiomyocyte  $F_{passive}$  has been found to be pathologically elevated in human HFpEF and heart failure with reduced ejection fraction (HFrEF), due to disturbed activity of PKA and PKG. While inhibition of PKC $\alpha$  activity has been suggested as a potential therapeutic target for hypertrophied hearts, boosting PKD enzyme activity in failing, overly stiff,

hearts could be beneficial for cardiomyocyte stiffness, similar to PKA, PKG, and ERK2 (Borbely et al., 2009; Raskin et al., 2012; van Heerebeek et al., 2012; Hamdani et al., 2013a, 2014; Kotter et al., 2013; Linke and Hamdani, 2014). A reduction in PKD-mediated titin phosphorylation, in turn, would increase  $F_{passive}$  and be detrimental to diastolic filling. However, a stiffer titin spring could speed up diastolic recoil and amplify some of the mechanosensory functions of titin.

### The PKD Substrate HSP27

The current study also showed that HSP27 content and phosphorylation is increased in human HCM hearts, a mechanism that might work to protect cardiomyocytes from

damage, as an established function of HSP27 is to prevent stress-induced protein aggregation and myocardial damage (Linke and Hamdani, 2014). The observed increase in HSP27 was associated with increased oxidative stress and increased content and activity of PKD, which also phosphorylates HSP27. PKD showed a polymer formation on EM, which indicates that PKD is oxidized. This may thus explain the beneficial *ex-vivo* effect of PKD on cardiomyocyte  $F_{\text{passive}}$  and indicates that perhaps increased PKD activity observed in HCM hearts is partially due to PKD oxidation as well—suggesting that by lowering oxidation we may improve cardiomyocyte function in a manner similar to administration of endogenous PKD *ex vivo*. PKD is an important downstream regulator of the oxidative stress response, and increased oxidative stress leads to the activation of different PKD isoforms and subsequent phosphorylation of HSP27 (Doppler et al., 2005; Stetler et al., 2012). In our study, phosphorylation of HSP27 was increased in HCM hearts, which is in line with previous findings showing that HSP27 phosphorylation prevents apoptosis by protecting cells against heat shock, apoptosis effectors, oxidative stress, and ischemia (Martin et al., 1997; Benjamin and McMillan, 1998; Knowlton et al., 1998; Yoshida et al., 1999; Dohke et al., 2006; Li et al., 2012). HSP27 is abundant in cardiac muscle cells, commonly localized to the Z-disk and I-band regions of the sarcomere, and involved in the protection of titin and intermediate filaments (Kotter et al., 2014; Linke and Hamdani, 2014). In HCM hearts, HSP27 showed a strongly altered localization away from the Z-disk and I-band, whereas in non-failing hearts, HSP27 was preferentially localized to the Z-disk and I-band. Whether the translocation of HSP27 depends on the altered phosphorylation status of HSP27 is still controversial (Mymrikov et al., 2011); altered phosphorylation of HSP27 at least did not alter the binding to titin domains (Kotter et al., 2014; Linke and Hamdani, 2014). HSP27 can function as an inhibitor of cell death upon its phosphorylation and dissociation to lower-molecular-weight oligomers, while the presence of the high-molecular-weight, non-phosphorylated form of HSP27 appears to be necessary for cellular protection against cardiac ischemia/reperfusion (Golenhofen et al., 2002, 2006; Kadono et al., 2006; Pinz et al., 2008). PKD specifically phosphorylates HSP27 in pancreatic cancer cells (Yuan and Rozenfurt, 2008) and endothelial cells (Evans et al., 2008). Phosphorylation of Ser82 is considered to be the main “effector” step for the shift from large molecular weight multimers to differentially functional oligomers. As regards titin, HSP27 specifically protects the unfolded Ig regions, but not the intrinsically disordered segments (N2Bus and PEVK), from aggregating under acidic stress (Kotter et al., 2014). The protective role of small HSPs on titin extensibility was also evident in earlier studies in which  $\alpha$ -B crystallin lowered the persistence length of the N2Bus segment and reduced the unfolding probability of the immunoglobulin domains flanking the N2Bus segment (Bullard et al., 2004). Isolated hearts lacking sHSPs (DKO) showed severe contractile dysfunction (Pinz et al., 2008), increased myocardial injury and resting tension (Golenhofen et al., 2006), accompanied by diastolic dysfunction in response to ischemia/reperfusion *ex vivo* (Pinz et al., 2008). This accords with our previous findings in isolated human cardiomyocytes in which under conditions

promoting titin aggregation (pre-stretch and acidic pH), passive stiffness was high in the absence of sHSPs but normal in the presence of sHSPs (Kotter et al., 2014). In our present work on human HCM cardiomyocytes, HSP27 lowered  $F_{\text{passive}}$  to the levels previously reported after administration of PKA and/or PKG (Borbely et al., 2005; Fukuda et al., 2005; Kruger et al., 2009; Falcao-Pires et al., 2011). In addition,  $F_{\text{passive}}$  fell to the level observed after PKD administration.

## CONCLUSION

Our findings have important therapeutic implications as they imply that drugs that balance PKD activity and restore HSP27 localization to the Z-disk and I band may show efficacy as a treatment for diastolic LV dysfunction related to high cardiomyocyte stiffness.

## DATA AVAILABILITY STATEMENT

All datasets generated for this study are included in the article/**Supplementary Material**.

## ETHICS STATEMENT

All animal procedures were performed in accordance with the guidelines of Charité Universitätsmedizin Berlin as well as Max-Delbrück Center for Molecular Medicine and were approved by the Landesamt für Gesundheit und Soziales (LaGeSo, Berlin, Germany) for the use of laboratory animals (permit number: G 0229/11) and followed the Principles of Laboratory Animal Care (NIH publication no. 86-23, revised 1985) as well as the current version of German Law on the Protection of Animals. The studies involving human participants were reviewed and approved by (St Vincent’s Hospital of Sydney, Australia, Human Research Ethics Committee; File number: H03/118; Title: Molecular Analysis of Human Heart Failure. The patients/participants provided their written informed consent to participate in this study.

## AUTHOR CONTRIBUTIONS

MH has generated all mass spectrometry and biochemistry data, analyzed all data, and has written the manuscript. DK has generated the confocal images and written the manuscript. ML has made the electron microscopy. SH and MK helped and supervised the mass spectrometry. ÁK performed mechanic experiments. ZP contributed to mechanics and rewrote the manuscript. KJ helped with re-analyzing the biochemistry data and rewrote the manuscript. PH provided the tissues. CD provided the human HCM biopsies. PR re-analyzed some data. AM re-analyzed the data and rewrote the manuscript. JF provided the Prkd1 mice and rewrote the manuscript. WL supervised and rewrote the manuscript. NH supervised, re-analyzed all data, performed mechanics, and wrote the manuscript.

## FUNDING

This work was supported by DFG (HA 7512/2-1) and FoRUM-Projekt (F765-13, F808N-14, and F882R-2017).

## ACKNOWLEDGMENTS

We gratefully acknowledge the technical assistance of Anja Vöge and Frauke De Pasquale. Also we acknowledge support

## REFERENCES

- Agah, R., Frenkel, P. A., French, B. A., Michael, L. H., Overbeek, P. A., and Schneider, M. D. (1997). Gene recombination in postmitotic cells. targeted expression of cre recombinase provokes cardiac-restricted, site-specific rearrangement in adult ventricular muscle *in vivo*. *J. Clin. Invest.* 100, 169–179.
- Aita, Y., Kurebayashi, N., Hirose, S., and Maturana, A. D. (2011). Protein kinase D regulates the human cardiac L-type voltage-gated calcium channel through serine 1884. *FEBS Lett.* 585, 3903–6. doi: 10.1016/j.febslet.2011.11.011
- Avkiran, M., Rowland, A. J., Cuello, F., and Haworth, R. S. (2008). Protein kinase d in the cardiovascular system: emerging roles in health and disease. *Circ. Res.* 102, 157–63. doi: 10.1161/CIRCRESAHA.107.168211
- Belin, R. J., Sumanda, M. P., Allen, E. J., Schoenfeld, K., Wang, H., Solaro, R. J., et al. (2007). Augmented protein kinase C- $\alpha$ -induced myofilament protein phosphorylation contributes to myofilament dysfunction in experimental congestive heart failure. *Circ. Res.* 101, 195–204. doi: 10.1161/CIRCRESAHA.107.148288
- Benjamin, I. J., and McMillan, D. R. (1998). Stress (heat shock) proteins: molecular chaperones in cardiovascular biology and disease. *Circ. Res.* 83, 117–132. doi: 10.1161/01.res.83.2.117
- Bishu, K., Hamdani, N., Mohammed, S. F., Kruger, M., Ohtani, T., Ogut, O., et al. (2011). Sildenafil and B-type natriuretic peptide acutely phosphorylate titin and improve diastolic distensibility *in vivo*. *Circulation* 124, 2882–2891. doi: 10.1161/CIRCULATIONAHA.111.048520
- Borbely, A., Falcao-Pires, I., van Heerebeek, L., Hamdani, N., Edes, I., Gavina, C., et al. (2009). Hypophosphorylation of the stiff N2B titin isoform raises cardiomyocyte resting tension in failing human myocardium. *Circ. Res.* 104, 780–786. doi: 10.1161/CIRCRESAHA.108.193326
- Borbely, A., van der Velden, J., Papp, Z., Bronzwaer, J. G., Edes, I., Stienen, G. J., et al. (2005). Cardiomyocyte stiffness in diastolic heart failure. *Circulation* 111, 774–781. doi: 10.1161/01.CIR.0000155257.33485.6D
- Bossuyt, J., Helmstadter, K., Wu, X., Clements-Jewery, H., Haworth, R. S., Avkiran, M., et al. (2008). Ca<sup>2+</sup>/calmodulin-dependent protein kinase II $\delta$  and protein kinase D overexpression reinforce the histone deacetylase 5 redistribution in heart failure. *Circ. Res.* 102, 695–702. doi: 10.1161/CIRCRESAHA.107.169755
- Bullard, B., Ferguson, C., Minajeva, A., Leake, M. C., Gautel, M., Labeit, D., et al. (2004). Association of the chaperone alphaB-crystallin with titin in heart muscle. *J. Biol. Chem.* 279, 7917–7924. doi: 10.1074/jbc.M307473200
- Cuello, F., Bardswell, S. C., Haworth, R. S., Yin, X., Lutz, S., Wieland, T., et al. (2007). Protein kinase D selectively targets cardiac troponin i and regulates myofilament Ca<sup>2+</sup> sensitivity in ventricular myocytes. *Circ. Res.* 100, 864–873. doi: 10.1161/01.RES.0000260809.15393.5a
- Dirx, E., Cazorla, O., Schwenk, R. W., Lorenzen-Schmidt, I., Sadayappan, S., Van Lint, J., et al. (2012). Protein kinase D increases maximal Ca<sup>2+</sup>-activated tension of cardiomyocyte contraction by phosphorylation of cMyBP-C-Ser315. *Am. J. Physiol. Heart Circ. Physiol.* 303, H323–H331. doi: 10.1152/ajpheart.00749.2011
- Dohke, T., Wada, A., Isono, T., Fujii, M., Yamamoto, T., Tsutamoto, T., et al. (2006). Proteomic analysis reveals significant alternations of cardiac small heat shock protein expression in congestive heart failure. *J. Card. Fail.* 12, 77–84. doi: 10.1016/j.cardfail.2005.07.006
- Doppler, H., Storz, P., Li, J., Comb, M. J., and Toker, A. (2005). A phosphorylation state-specific antibody recognizes Hsp27, a novel substrate of protein kinase D. *J. Biol. Chem.* 280, 15013–15019. doi: 10.1074/jbc.C400575200

by the DFG Open Access Publication Funds of the Ruhr-Universität Bochum.

## SUPPLEMENTARY MATERIAL

The Supplementary Material for this article can be found online at: <https://www.frontiersin.org/articles/10.3389/fphys.2020.00240/full#supplementary-material>

- Evans, I. M., Britton, G., and Zachary, I. C. (2008). Vascular endothelial growth factor induces heat shock protein (HSP) 27 serine 82 phosphorylation and endothelial tubulogenesis via protein kinase D and independent of p38 kinase. *Cell. Signal.* 20, 1375–1384. doi: 10.1016/j.cellsig.2008.03.002
- Falcao-Pires, I., Hamdani, N., Borbely, A., Gavina, C., Schalkwijk, C. G., van der Velden, J., et al. (2011). Diabetes mellitus worsens diastolic left ventricular dysfunction in aortic stenosis through altered myocardial structure and cardiomyocyte stiffness. *Circulation* 124, 1151–1159. doi: 10.1161/CIRCULATIONAHA.111.025270
- Fielitz, J., Kim, M. S., Shelton, J. M., Qi, X., Hill, J. A., Richardson, J. A., et al. (2008). Requirement of protein kinase D1 for pathological cardiac remodeling. *Proc. Natl. Acad. Sci. U.S.A.* 105, 3059–3063. doi: 10.1073/pnas.0712265105
- Franssen, C., Chen, S., Unger, A., Korkmaz, H. I., De Keulenaer, G. W., Tschope, C., et al. (2016). Myocardial microvascular inflammatory endothelial activation in heart failure with preserved ejection fraction. *JACC Heart Fail.* 4, 312–324. doi: 10.1016/j.jchf.2015.10.007
- Fukuda, N., Wu, Y., Nair, P., and Granzier, H. L. (2005). Phosphorylation of titin modulates passive stiffness of cardiac muscle in a titin isoform-dependent manner. *J. Gen. Physiol.* 125, 257–271. doi: 10.1085/jgp.200409177
- Golenhofen, N., Arbeiter, A., Koob, R., and Drenckhahn, D. (2002). Ischemia-induced association of the stress protein alpha B-crystallin with I-band portion of cardiac titin. *J. Mol. Cell. Cardiol.* 34, 309–319. doi: 10.1006/jmcc.2001.1513
- Golenhofen, N., Redel, A., Wawrousek, E. F., and Drenckhahn, D. (2006). Ischemia-induced increase of stiffness of alphaB-crystallin/HSPB2-deficient myocardium. *Pflugers Arch.* 451, 518–525. doi: 10.1007/s00424-005-1488-1
- Hamdani, N., Bishu, K. G., von Frieling-Salewsky, M., Redfield, M. M., and Linke, W. A. (2013a). Deranged myofilament phosphorylation and function in experimental heart failure with preserved ejection fraction. *Cardiovasc. Res.* 97, 464–471. doi: 10.1093/cvr/cvs353
- Hamdani, N., Hervent, A.-S., Vandekerckhove, L., Matheeußen, V., Demolder, M., Baerts, L., et al. (2014). Left ventricular diastolic dysfunction and myocardial stiffness in diabetic mice is attenuated by inhibition of dipeptidyl peptidase 4. *Cardiovasc. Res.* 104, 423–431. doi: 10.1093/cvr/cvu223
- Hamdani, N., Krysiak, J., Kreusser, M. M., Neef, S., Dos Remedios, C. G., Maier, L. S., et al. (2013b). Crucial role for Ca<sup>2+</sup>/calmodulin-dependent protein kinase-II in regulating diastolic stress of normal and failing hearts via titin phosphorylation. *Circ. Res.* 112, 664–674. doi: 10.1161/CIRCRESAHA.111.300105
- Harrison, B. C., Kim, M. S., van Rooij, E., Plato, C. F., Papst, P. J., Vega, R. B., et al. (2006). Regulation of cardiac stress signaling by protein kinase d1. *Mol. Cell. Biol.* 26, 3875–3888. doi: 10.1128/MCB.26.10.3875-3888.2006
- Haworth, R. S., Cuello, F., Herron, T. J., Franzen, G., Kentish, J. C., Gautel, M., et al. (2004). Protein kinase D is a novel mediator of cardiac troponin i phosphorylation and regulates myofilament function. *Circ. Res.* 95, 1091–1099. doi: 10.1161/01.RES.0000149299.34793.3c
- Hayashi, A., Seki, N., Hattori, A., Kozuma, S., and Saito, T. (1999). PKC $\nu$ , a new member of the protein kinase C family, composes a fourth subfamily with PKC $\mu$ . *Biochim. Biophys. Acta* 1450, 99–106. doi: 10.1016/s0167-4889(99)00040-3
- Hidalgo, C., Hudson, B., Bogomolova, J., Zhu, Y., Anderson, B., Greaser, M., et al. (2009). PKC phosphorylation of titin's PEVK element: a novel and conserved pathway for modulating myocardial stiffness. *Circ. Res.* 105, 631–638. doi: 10.1161/CIRCRESAHA.109.198465

- Johannes, F. J., Prestle, J., Eis, S., Oberhagemann, P., and Pfizenmaier, K. (1994). PKC $\alpha$  is a novel, atypical member of the protein kinase C family. *J. Biol. Chem.* 269, 6140–6148.
- Kadono, T., Zhang, X. Q., Srinivasan, S., Ishida, H., Barry, W. H., and Benjamin, I. J. (2006). CRYAB and HSPB2 deficiency increases myocyte mitochondrial permeability transition and mitochondrial calcium uptake. *J. Mol. Cell. Cardiol.* 40, 783–789. doi: 10.1016/j.yjmcc.2006.03.003
- Kim, M. S., Fielitz, J., McAnally, J., Shelton, J. M., Lemon, D. D., McKinsey, T. A., et al. (2008). Protein kinase D1 stimulates MEF2 activity in skeletal muscle and enhances muscle performance. *Mol. Cell. Biol.* 28, 3600–3609. doi: 10.1128/MCB.00189-08
- Knowlton, A. A., Kapadia, S., Torre-Amione, G., Durand, J. B., Bies, R., Young, J., et al. (1998). Differential expression of heat shock proteins in normal and failing human hearts. *J. Mol. Cell. Cardiol.* 30, 811–818. doi: 10.1006/jmcc.1998.0646
- Kostenko, S., and Moens, U. (2009). Heat shock protein 27 phosphorylation: kinases, phosphatases, functions and pathology. *Cell. Mol. Life Sci.* 66, 3289–3307. doi: 10.1007/s00018-009-0086-3
- Kotter, S., Gout, L., Von Frieling-Salewsky, M., Muller, A. E., Helling, S., Marcus, K., et al. (2013). Differential changes in titin domain phosphorylation increase myofibrillar stiffness in failing human hearts. *Cardiovasc. Res.* 99, 648–656. doi: 10.1093/cvr/cvt144
- Kotter, S., Unger, A., Hamdani, N., Lang, P., Vorgerd, M., Nagel-Steger, L., et al. (2014). Human myocytes are protected from titin aggregation-induced stiffening by small heat shock proteins. *J. Cell. Biol.* 204, 187–202. doi: 10.1083/jcb.201306077
- Kruger, M., Kotter, S., Grutzner, A., Lang, P., Andresen, C., Redfield, M. M., et al. (2009). Protein kinase G modulates human myocardial passive stiffness by phosphorylation of the titin springs. *Circ. Res.* 104, 87–94. doi: 10.1161/CIRCRESAHA.108.184408
- Kruger, M., and Linke, W. A. (2006). Protein kinase-A phosphorylates titin in human heart muscle and reduces myofibrillar passive tension. *J. Muscle Res. Cell Motil.* 27, 435–444. doi: 10.1007/s10974-006-9090-5
- Kruger, M., Moser, M., Ussar, S., Thievensen, I., Lubert, C. A., Forner, F., et al. (2008). SILAC mouse for quantitative proteomics uncovers kindlin-3 as an essential factor for red blood cell function. *Cell* 134, 353–364. doi: 10.1016/j.cell.2008.05.033
- Li, Z., Liu, X., Zhao, Z., and Liu, W. (2012). [Heat shock protein 27 enhances the inhibitory effect of influenza A virus NS1 on the expression of interferon-beta]. *Sheng Wu Gong Cheng Xue Bao* 28, 1205–1215.
- Linke, W. A., and Hamdani, N. (2014). Gigantic business: titin properties and function through thick and thin. *Circ. Res.* 114, 1052–1068. doi: 10.1161/CIRCRESAHA.114.301286
- Martin, J. L., Mestril, R., Hilal-Dandan, R., Brunton, L. L., and Dillmann, W. H. (1997). Small heat shock proteins and protection against ischemic injury in cardiac myocytes. *Circulation* 96, 4343–4348. doi: 10.1161/01.cir.96.12.4343
- Mymrikov, E. V., Seit-Nebi, A. S., and Gusev, N. B. (2011). Large potentials of small heat shock proteins. *Physiol. Rev.* 91, 1123–1159. doi: 10.1152/physrev.00023.2010
- Nichols, C. B., Chang, C. W., Ferrero, M., Wood, B. M., Stein, M. L., Ferguson, A. J., et al. (2014). beta-adrenergic signaling inhibits Gq-dependent protein kinase D activation by preventing protein kinase D translocation. *Circ. Res.* 114, 1398–1409. doi: 10.1161/CIRCRESAHA.114.303870
- Pinz, I., Robbins, J., Rajasekaran, N. S., Benjamin, I. J., and Ingwall, J. S. (2008). Unmasking different mechanical and energetic roles for the small heat shock proteins CryAB and HSPB2 using genetically modified mouse hearts. *FASEB J.* 22, 84–92. doi: 10.1096/fj.07-8130com
- Raskin, A., Lange, S., Banares, K., Lyon, R. C., Zieseniss, A., Lee, L. K., et al. (2012). A novel mechanism involving four-and-a-half LIM domain protein-1 and extracellular signal-regulated kinase-2 regulates titin phosphorylation and mechanics. *J. Biol. Chem.* 287, 29273–29284. doi: 10.1074/jbc.M112.372839
- Sin, Y. Y., and Baillie, G. S. (2012). Protein kinase D in the hypertrophy pathway. *Biochem. Soc. Trans.* 40, 287–289. doi: 10.1042/BST20110626
- Stetler, R. A., Gao, Y., Zhang, L., Weng, Z., Zhang, F., Hu, X., et al. (2012). Phosphorylation of HSP27 by protein kinase D is essential for mediating neuroprotection against ischemic neuronal injury. *J. Neurosci.* 32, 2667–2682. doi: 10.1523/JNEUROSCI.5169-11.2012
- Sturany, S., van Lint, J., Muller, F., Wilda, M., Hameister, H., Hocker, M., et al. (2001). Molecular cloning and characterization of the human protein kinase D2, a novel member of the protein kinase D family of serine threonine kinases. *J. Biol. Chem.* 276, 3310–3318. doi: 10.1074/jbc.M008719200
- Valverde, A. M., Sinnett-Smith, J., Van Lint, J., and Rozengurt, E. (1994). Molecular cloning and characterization of protein kinase D: a target for diacylglycerol and phorbol esters with a distinctive catalytic domain. *Proc. Natl. Acad. Sci. U.S.A.* 91, 8572–8576. doi: 10.1073/pnas.91.18.8572
- van Heerebeek, L., Hamdani, N., Falcao-Pires, I., Leite-Moreira, A. F., Begieneman, M. P., Bronzwaer, J. G., et al. (2012). Low myocardial protein kinase G activity in heart failure with preserved ejection fraction. *Circulation* 126, 830–839. doi: 10.1161/CIRCULATIONAHA.111.076075
- Van Lint, J. V., Sinnett-Smith, J., and Rozengurt, E. (1995). Expression and characterization of PKD, a phorbol ester and diacylglycerol-stimulated serine protein kinase. *J. Biol. Chem.* 270, 1455–1461. doi: 10.1074/jbc.270.3.1455
- Vega, R. B., Harrison, B. C., Meadows, E., Roberts, C. R., Papst, P. J., Olson, E. N., et al. (2004). Protein kinases C and D mediate agonist-dependent cardiac hypertrophy through nuclear export of histone deacetylase 5. *Mol. Cell. Biol.* 24, 8374–8385. doi: 10.1128/MCB.24.19.8374-8385.2004
- Yamasaki, R., Wu, Y., McNabb, M., Greaser, M., Labeit, S., and Granzier, H. (2002). Protein kinase A phosphorylates titin's cardiac-specific N2B domain and reduces passive tension in rat cardiac myocytes. *Circ. Res.* 90, 1181–1188. doi: 10.1161/01.res.0000021115.24712.99
- Yoshida, N., Kristiansen, A., and Liberman, M. C. (1999). Heat stress and protection from permanent acoustic injury in mice. *J. Neurosci.* 19, 10116–10124.
- Yuan, J., and Rozengurt, E. (2008). PKD, PKD2, and p38 MAPK mediate Hsp27 serine-82 phosphorylation induced by neurotensin in pancreatic cancer PANC-1 cells. *J. Cell. Biochem.* 103, 648–662. doi: 10.1002/jcb.21439
- Zhao, D., Gao, Y., Wang, W., Pei, H., Xu, C., Zhao, Z. (2019). PKD deletion promotes autophagy and inhibits hypertrophy in cardiomyocyte. *Exp. Cell Res.* 386:111742. doi: 10.1016/j.yexcr.2019.111742
- Zhao, D., Wang, W., Wang, H., Peng, H., Liu, X., Guo, W., et al. (2017). PKD knockdown inhibits pressure overload-induced cardiac hypertrophy by promoting autophagy via AKT/mTOR pathway. *Int. J. Biol. Sci.* 13, 276–285. doi: 10.7150/ijbs.17617

**Conflict of Interest:** SH was employed by the company Sanofi-Aventis Deutschland GmbH Industriepark Höchst.

The remaining authors declare that the research was conducted in the absence of any commercial or financial relationships that could be construed as a potential conflict of interest.

Copyright © 2020 Herwig, Kolijn, Lódi, Hölper, Kovács, Papp, Jaquet, Haldenwang, Dos Remedios, Reusch, Mügge, Krüger, Fielitz, Linke and Hamdani. This is an open-access article distributed under the terms of the Creative Commons Attribution License (CC BY). The use, distribution or reproduction in other forums is permitted, provided the original author(s) and the copyright owner(s) are credited and that the original publication in this journal is cited, in accordance with accepted academic practice. No use, distribution or reproduction is permitted which does not comply with these terms.